CEBAF PROPOSAL COVER SHEET

This Proposal must be mailed to:

CEBAF
Scientific Director's Office
12000 Jefferson Avenue
Newport News, VA 23606

and received on or before OCTOBER 30, 1989

A. TITLE: Electromagnetic Production of Hyperons

B. CONTACT PERSON: Reinhard Schumacher

ADDRESS, PHONE AND BITNET:

Dept. of Physics, Carnegie Mellon Univ.
Pittsburgh, PA 15213
REINHARD@CMPHYSME

C. THIS PROPOSAL IS BASED ON A PREVIOUSLY SUBMITTED LETTER OF INTENT

☒ YES
☐ NO

IF YES, TITLE OF PREVIOUSLY SUBMITTED LETTER OF INTENT

Experimental Study of Strangeness Photoproduction

D. ATTACH A SEPARATE PAGE LISTING ALL COLLABORATION MEMBERS AND THEIR INSTITUTIONS

==========

(CEBAF USE ONLY)

Letter Received 10-30-89

Log Number Assigned PR-89-004

By KES

contact: Schumacher

CMU-DOE/ER/40315-170
CMU/ME - 014/89

PROPOSAL
to the C.E.B.A.F. Program Advisory Committee

ELECTROMAGNETIC PRODUCTION OF HYPERONS

Members of the CLAS collaboration particularly interested in the measurements in this proposal:

Peter D. Barnes, Gregg Franklin, Brian Quinn, and Reinhard A. Schumacher (Spokesman)
Department of Physics
Carnegie Mellon University
Pittsburgh, PA 15213

Hall Crannell and Daniel I. Sober
Department of Physics
The Catholic University of America
Washington D.C. 20064

Richard Arndt, David Jenkins, David Roper, and Ron Workman
Department of Physics
Virginia Polytechnic Institute and State University
Blacksburg, VA 24061

Bernhard Mecking
C.E.B.A.F.
Newport News, VA 23606

Larry Dennis and Kirby Kemper
Department of Physics
Florida State University
Tallahassee, FL 32306

Jen-Chieh Peng and Michael J. Leitch
Los Alamos National Laboratory
Los Alamos, N.M. 87545

It is proposed to use the CEBAF Large Acceptance Spectrometer (CLAS) in a series of measurements to study the photo- and electro-production of the low-mass strange baryons. The creation of $s\bar{s}$ quark pairs adds a new degree of freedom to baryon spectroscopy, which is an approach complimentary to the study of non-strange baryon resonances. Electromagnetic hyperon production can be compared with hadron-induced reactions, avoiding, for example, the complications of initial state interactions. Surprisingly few data on electromagnetic hyperon production exist, and this has hampered progress on the theoretical side. For real photoproduction of the Λ and Σ^0, theories developed in terms of baryon and meson exchanges have been unable to resolve several basic inconsistencies in comparing to data and to each other. Y^* photoproduction has scarcely been measured, and neither has hyperon electroproduction. Better understanding of hyperon photo- and electro-production is essential to hypernuclear studies, which have considerable sensitivity to details of the elementary interaction.

Two "first-round" measurements which can be done with the CLAS and the proposed photon tagger have been selected for detailed discussion. They are 1) the elementary photoproduction of Λ hyperons, measuring the polarization of the Λ as well as the differential cross section from threshold to about 1.8 GeV; and 2) the elementary photoproduction of Σ^0 hyperons under kinematic conditions similar to the Λ's. The differential cross section for reaction (1) is only moderately well established, and the addition of polarization data will enable significant progress in the understanding of the elementary amplitudes of strangeness photoproduction. Reaction (2) has rarely been measured due the lack of appropriate tagged photon beams, and should further constrain the spin–isospin structure of photoproduction models. In addition, we propose to make exploratory measurements of excited hyperon production, Λ and Σ^0 production at energies above 1.8 GeV, and electro-production of hyperons.

With a 5% overall CLAS momentum and geometrical acceptance for a three-body (K^+,π^-,p) final state, and assuming a $1 gm/cm^2$ hydrogen target with 2×10^7 γ/sec incident, one can expect to detect about 1400 events/hour for each of the elementary production reactions for polarization measurements. Twice this rate is achievable if the (kinematically redundant) pion is not detected. Data for both Λ and Σ^0 reactions can be accumulated simultaneously.

Physics Motivation

Studies of systems with one or more s-quarks add to our understanding of fundamental two particle interactions by providing an opportunity to extend models developed for N-N, π–N, and γ-N (i.e. non-strange) interactions. New experiments measuring the elementary photoproduction of strange particles will result in better determination of the hyperon-nucleon coupling constants, and of the proper formulation of the strangeness producing interaction. Since the proton from the decay $\Lambda \rightarrow p + \pi^-$ is emitted in a direction correlated with the direction of the Λ spin, information about the Λ polarization is easily obtained in a large solid angle detector. This "self-analyzing" property of the Λ allows spin-physics to be extracted which may rival the data from much more complex experiments performed for the N-N system. Improved understanding of the elementary strangeness photoproduction operator will benefit studies of hypernuclear photoproduction, since there can be considerable sensitivity of predicted hypernuclear production cross section to the details of the elementary interaction.

The associated production of strange particles (reactions in which an S= +1 particle is produced along with an associated S= −1 particle) has been studied with reactions such as $\pi^- + p \rightarrow K^o + \Lambda$ [1], $p + \bar{p} \rightarrow \Lambda + \bar{\Lambda}$ [2], and $p + p \rightarrow \Lambda + X$ [3]. Figure 1 shows the quark flow diagrams for some of these reactions. The final state hyperons formed through these reactions have been found to be strongly polarized. The cause of this polarization may be partially due to elementary $s\bar{s}$ quark pair production and partially due to initial and final state interactions. The photoproduction of Λ–K and Σ–K pairs are reactions well suited to study polarization effects, since initial state interactions are absent.

In this proposal we will focus on real photon measurements, with the intention of undertaking only exploratory electroproduction measurements at first, in preparation for a more extensive second round of experiments. Great improvement in the existing data can be obtained at CEBAF through strangeness production experiments with either real or virtual photons. Virtual photoproduction (*i.e.* doing (e,e'K)X) allows exploration of the full (Q^2,ν) response structure of the reaction. Historically, very few electroproduction data have been obtained [4], while the real photoproduction data (discussed below) are more numerous and still not well understood. The advantage of studying real photoproduction over electroproduction is that only four rather than six complex amplitudes need to be considered. Real photoproduction will be experimentally more straightforward than electroproduction also, because one less particle needs to be detected in the multi-particle detector, while rate problems should be less severe using a real photon beam.

Reaction 1): The reaction $\gamma + p \rightarrow \Lambda + K^+$ has been studied since the late fifties [5], and received considerable experimental and theoretical attention in the 60's and early 70's. The differential cross section is moderately well established from threshold (at 911 MeV) up to 1.4 GeV, while the polarization of the Λ has been measured at only a few angles and energies , and typically with large error bars. Figures 2 and 3 give overviews of the existing differential cross section data and polarization data[6],[7],[8]. Note that the polarization data shown in Figure 3a, which are for a kaon c.m. angle of $90^\circ \pm 5^\circ$, represent well over half of the data points ever measured. Other data points are scattered in angle and energy (Figure 3c). One sees that while the differential cross section is moderately well established, little more than the sign of the polarization is known.

Presently, no theories of strangeness photoproduction inspired directly by the quark model exist. One might expect such models to be constructible, as they have for the reaction $p\bar{p} \rightarrow \Lambda\bar{\Lambda}$, for example [9]. Traditional calculations have been undertaken using Feynman diagrams involving the exchange of mesons and baryons. The Born term graphs for the s, t, and u channels of Λ photoproduction are shown in Figure 4. In addition to the graphs involving the exchange of ground state baryons and mesons, one must generally include graphs with low-lying N* (s-channel), Y* (u-channel), and K* (t-channel) intermediate states. Partly due to a lack of sufficient good data, uncertainty has persisted for many years over the proper formulation of the interaction, particularly regarding which resonances should be included and the form of some of the couplings (pseudo-vector *vs* pseudo-scalar) in the models [24]. One consequence of this is a long-standing uncertainty about the correct values of the basic coupling constants $g_{K\Lambda N}$ and $g_{K\Sigma N}$. Table I shows a compilation of $g_{K\Lambda N}$ values obtained over the years. From this table one can see that the older analyses of photoproduction data have produced values for $g_{K\Lambda N}$ roughly a factor of two smaller than those obtained from hadronic data (from analysis of KN scattering data, for example), and that there is poor agreement among the theoretical approaches.

Recent authors have attempted to address the source of these problems. Adelseck and Wright [20] found that including $K_1(1280)$ (formerly Q(1280)) exchange in the t-channel increased $g_{\Lambda KN}$ to the hadronic value. Tanabe, Kohno, and Bennhold [21], on the other hand, pointed out the necessity of including K^++Λ final state correlations explicitly. By including a partial wave dependent absorptive factor on top of the usual Born and resonance terms, they fit the total cross section data at higher energies (above 1.5 GeV) and claim to get the hadronic-reaction value for $g_{K\Lambda N}$ (see Figure 5). Workman [22] [23] has recently emphasized the model dependence of results obtained by adding or leaving out nucleon and hyperon resonances in a more or less *ad hoc* fashion, as well as the fact that error estimates on the extracted coupling constants have generally been neglected. He finds that the Born couplings are not stable against the addition of

higher resonances. Cohen[24] has found that taking the couplings derived from photoproduction and recalculating hadronic reactions such as low energy KN scattering unexpectedly produces *better* agreement with data than the "standard" hadronic values. He questions, however, the validity of the diagrammatic models used in all studies on the grounds of the largeness of the kaon mass relative to the nucleon mass, and the resulting non-applicability of certain low-energy theorems. Hence the theoretical situation is not at all settled.

Various authors [6],[7],[21],[22],[25] have pointed out that if better Λ polarization data were available, progress could be made in this field. Figure 3a), for example, shows the older analysis of Renard [7] which clearly indicates the sensitivity of his model to Λ polarization data: the hatched region shows the range of predictions due to reasonable variations of the couplings $g_{\Lambda KN}$ and $g_{\Sigma KN}$ (compare to Figure 2). Figure 3b) is from the newer analysis of Adelseck and Wright [20] (same data with opposite sign convention), showing again the poor quality of the present data. Figure 3c) shows Λ polarization data as a function of angle with a partial wave analysis calculation[8], once again showing how sparse the existing data are. Apart from better differential cross section data, Λ polarization measurements would be the principal contribution of new experiments at CEBAF, which would be designed to look for the self-analyzing decay of the Λ into $\pi^- p$ in coincidence with the kaon which tags production of the Λ. This will be possible with the CLAS, since it will be capable of detecting the Λ decay products as well as the kaons.

In the rest frame of the Λ, the weak decay $\Lambda \rightarrow \pi^- p$ emits the nucleon preferentially along the direction of the Λ spin. For a sample of hyperons with polarization P, the decay yields a distribution $I(\theta_p) = I_o(1 + \alpha P \cos\theta_p)$ where α is the weak decay asymmetry parameter ($\alpha = 0.642 \pm 0.013$) and θ_p is the angle between the normal to the production reaction plane and the nucleon momentum. For given photon energy and kaon angle bins, approximately 950 Λ decays must be observed to obtain a $\delta P = 0.05$ determination of the polarization, for typical polarization values of about $P \approx 0.3$.

One can point out that CEBAF will eventually provide polarized hydrogen targets and polarized photon beams. Thus, one can imagine experiments measuring a wide range of polarization observables in the Λ production reaction. Adelseck and Saghai [25] have recently itemized the possible combinations of photon, target, and lambda polarization measurements which can be made. Figure 6 shows some of their predictions for the asymmetry observables P, the lambda polarization (discussed above), Σ the kaon phi-angle asymmetry using linearly polarized photons, and C_x, the lambda asymmetry when circularly polarized photons are used. The three curves differ in that the $g_{\Lambda KN}$ coupling has been varied by $\pm 10\%$ about the "best" value, and one sees consider-

able sensitivity to the polarization variables. Workman [26] has also studied the sensitivity of several models to the only existing target polarization measurement [27] and concludes that measurements of these observables will be useful in discriminating among models. The Σ (linearly polarized) asymmetry may be straightforward to measure if the CLAS photon tagger is equipped with a crystal radiator for coherent bremsstrahlung work.

An area of application of the strangeness photoproduction operator is in the photoproduction of hypernuclear states. For example, one recent work has indicated a considerable degree of sensitivity to the details of the elementary operator when embedding it in a nuclear medium [28]. Figure 7 shows the predicted $^{16}O(\gamma,K^+)^{16}_{\Lambda}N$ cross section for three formulations of the elementary interaction. Differences of up to an order of magnitude are seen.

Reaction 2): We now consider the elementary photoproduction of the Σ^o hyperon. Figure 8 shows the few differential cross section data which exist[7],[29] ; the threshold is E_γ = 1046 MeV. These data are sparse because (traditional) untagged bremsstrahlung beam experiments can only separate the production of the Σ^o from the Λ by the difficult method of bremsstrahlung endpoint fitting. The bremsstrahlung difference method has also been used, but it is slow and cumbersome. The tagged photon method offers adequate missing mass resolution to resolve the Σ^o, and can cover a wide photon energy range simultaneously, making it attractive to measure Λ and Σ^o production simultaneously. Indeed, the higher mass hyperon states such as the $\Lambda(1405)$, $\Lambda(1520)$, and $\Sigma(1385)$ can also be produced in one setting of the CLAS detector. (We are requesting some time for exploratory measurements of the production cross sections of these states.) As discussed below, the missing mass resolution for the Λ and Σ^o in the CLAS is about 8.5 MeV FWHM.

The Λ and Σ^o hyperons are in the same spin-parity octet, and are related at the quark level by spin flips of two quarks. The production ratio of these two hyperons is predicted by spin-flavor SU(6) to be $\sigma(\gamma p \rightarrow K^+\Sigma^o) / \sigma(\gamma p \rightarrow K^+\Lambda) = 1 / 3$, while experiment yields a ratio of about unity [30] away from threshold. Since the Σ^o has isospin 1, rather than isospin 0 like the Λ, the isospin 3/2 Δ resonances can play a role in the production process. The fact that additional terms are needed to describe Σ^o photoproduction points out the desirability for more and better data on this reaction. Σ^o photoproduction has been treated theoretically by Renard[7] and Bennhold[31]. Also, no polarization information exists at all for Σ^o production. Because the Σ^o decays 100% via an M1 transition to the Λ, a measurement of the Λ polarization also measures the polarization of the Σ^o. The relationship is that $P_\Lambda = -1/3\ P_{\Sigma o}$.

Experimental Requirements

The continuous beam at CEBAF and the CLAS detector with the photon tagger will make it possible to obtain a large quantity of new, kinematically complete data on hyperon photo-production in an efficient manner. The tagger is needed to establish the kinematics of the initial state, and the fully-instrumented CLAS will be needed to detect and record the multi-particle final states.

The common experimental feature of the reactions discussed above is the requirement to identify strangeness production in the on-line trigger to filter out the copious non-strange events. One can exploit the fact that the production and decay in the above reactions are all two-body interactions, so that one-to-one mapping between kinematic variables exists (for example between kaon angle and kaon momentum). Strictly, these measurements could be made with a non-magnetic imaging detector which records only the tracks of all charged final state particles. An example of this approach is the PS185 experiment at LEAR [2]. The momentum information obtained using a magnetic detector is obtained at the added cost of reconstructing curved tracks and some loss of "dynamic range" where low momentum particles do not reach the trigger counters. The advantage of a magnetic detector is the redundancy checks that the momentum information provides in analyzing the data.

Another useful kinematic feature in these measurements is the fact that the Λ has a decay length of several centimeters ($c\tau$=7.9cm). This opens the possibility of using the neutral "V" to signal the production of strange particles. The vertex defined by the $\Lambda \rightarrow \pi^- + p$ decay will be spatially separated by distances on the order of centimeters from the track of the K^+. Making a cut on a minimum distance between the kaon track and the Λ vertex can be used to select events with strange particles. Certainly the off-line analysis will use this technique to select the "good" events. With sufficient on-line processing power it may also be possible to use this method on line as well. Note that with increasing momentum, where kaon time-of-flight identification will become increasingly difficult, the Λ will also have an increasing decay length in the lab frame, making the latter method more useful in identifying strangeness production. Reactions producing the $\Lambda(1405)$, $\Lambda(1520)$ and the $\Sigma(1385)$ hyperons will also be in the tagged photon data set. These resonances will decay either strongly or electromagnetically at the production vertex; however, the neutral "V" identification method can be used to detect weak decay vertex of the $\Lambda(1116)$, into which all the hyperon resonances eventually decay.

It should be emphasized that the reactions outlined above do not require separate data taking runs. In fact, the data for these reactions will be recorded simultaneously, with the same on-line strangeness production trigger.

The main technical feasibility issues are as follows:

1) Production Rates

The total production cross section for Λ photoproduction is close to 1μb in the E_γ energy range between 1 and 2 GeV. For a 1.0 gram/cm^2 liquid hydrogen target (14 cm in length) and a total photon tagging rate (over all energies) of 10MHz, one obtains a raw production rate of 6 Λ/K events per second. For inclusive kaon measurements, such as of the unpolarized differential cross section, this results in over 21,600 produced kaons per hour. For Λ production we are looking for the charged decay mode $\Lambda \rightarrow p\,\pi^-$, which has a 64% branch. Thus, the effective detectable Λ photoproduction rate is 4 per second before considering the detector acceptance. The Σ^0 production rate is between 2/3 and unity times the Λ rate. Thus the total production rate for the two low-lying hyperons, Λ and Σ^0, detected in the ($K^+\,\pi^-\,p$) or ($K^+\,p$) final states would be about 23,000 hyperons/hour, integrated over all tagged photon energies, which is sufficient to do the measurements outlined above.

2) Photon beam

Photon tagging rates of 10^7/sec (perhaps several times this) are expected at the CEBAF facility. It is expected that the tagger will not limit the coincidence timing since each photon will be localizable to a beam microstructure bucket of intrinsic duration of a few hundred picoseconds. For an average tagging rate of 10^7/sec and for an estimated 20 nanosecond resolving time, there is a 20% pile-up probability at the first trigger level when correlating an event in the CLAS with a hit in the tagging hodoscope. Off-line event reconstruction should improve the start-time estimate of the CLAS considerably, but it is too soon to predict the eventual performance of the device. The tagged photon energy resolution should be about 5 MeV to be comparable to other contributions to the hyperon missing mass resolution in the (γ,K) arm of the experiment. (See below, Figure 18.) The design for a photon tagger suitable for these measurements has been developed by the Photon Tagging Working Group[32]. Without a full-power beam dump under the CLAS, untagged bremsstrahlung measurements will not be possible; for the present measurements, an untagged photon beam could have been used at energies below the Σ threshold.

3) Target

Our rate estimates are based on a 1gm/cm^2 hydrogen target, which would be 14 cm long in liquid form. The target must have thin walls in essentially all directions to avoid blind spots in the acceptance. In practice, the target will have a flange on the upstream side, where the particle rates are very low, from which the target vessel is cantilevered forward. The measurements discussed here could be done with an even longer target since a "non-interacting" photon beam is being used; for example a 30cm target would in principle work well. The reactions studied here are forward peaked in the lab. The target will be mounted in way that allows it to be shifted upstream from the nominal detector center in order to increase the acceptance at very forward angles.

4) Acceptance of the Detector

Consider the reaction $\gamma + p \rightarrow K^+ + \Lambda$. We initially assume isotropic production of kaons in the γp center-of-mass frame and let the lambdas decay isotropically in their center-of-mass frame. Figure 9 shows the laboratory frame 3-body phase space of the detected particles for a photon energy of 1.1 GeV. Note that the heavier particles are strongly forward peaked (below about 60^o) and that the pions have only a slight tail to large angles. This illustrates the requirement that the CLAS must have very good forward angle coverage. The case for $E_\gamma = 1.8$ GeV is shown in Figure 10. The kaons as well as the pions can reach backward angles at this energy.

The acceptance of the CLAS for strangeness photoproduction was studied using the CEBAF Monte Carlo program called FASTMC[33]. It is a simple model of the detector which parameterizes the momentum and angle acceptance of individual tracks, as well as the single-track momentum resolution as a function of angle and momentum. Figure 11 shows the percentage of three-body (K,π^-,p) final states accepted by the CLAS as a function of photon energy using the "canonical" acceptance functions in the model: positive particles bend inward and the magnetic field is at full strength. The curves correspond to different "good event" requirements: all three require the kaon be detected in the scintillators; the low curve requires the π^- and p to reach the scintillators, the middle curve that the π^- and p to reach Region 2, and the high acceptance curve that the π^- and p to reach only as far as Region 1. Note that the acceptance in the threshold region vanishes.

By modifying FASTMC to consider the CLAS acceptance for lower values of the magnetic field we found that a much better configuration is obtained with $B = 0.2\ B_0$, or one fifth of the nominal field, as show in Figure 12. The best acceptance below 1.8 GeV is between 5% and 10%. The curves have the same meaning as above, with the best acceptance when kaons are used to trigger in the outer scintillators and the pions and protons are detected only in Region 1.

Reversing polarity on the magnet produced a slightly less good result because the low momentum negative pions were then bent inward and therefore lost more often. We note that in fact one could run these measurements with the magnet switched completely off, since all interaction steps are given by two-body kinematics, and hence the reactions are completely determined even if only the angles of all the final state particles are measured. It was found that the acceptance did not increase, however, when reducing the field from 0.2 of nominal to zero. For redundancy, we plan to run the experiment at the lowest possible field setting consistent with maintaining adequate momentum resolution.

If the condition that all three final state particles are detected is relaxed, then the acceptance will typically increase. The Λ polarization can still be measured if only the proton is detected, hence in these measurements the low-momentum pion could be left undetected. Figure 13 shows the CLAS acceptance then only the K^+ and p are detected. At 1.5 GeV the acceptance increases from 12% to 20%, for example, if the pion is not detected. Unlike the previous case, it now makes no difference if the magnet is run at full field or 0.2 of full field. Also at *low* field it makes no difference in the acceptance if the positive particles bend in or out. We plan to run with a trigger, therefore, which accepts those two-body final states containing a detected kaon and a proton, but not necessarily containing a detected pion.

It is clear that a 10% typical acceptance in the threshold region is rather small, and that these measurements require that all six sectors of the detector be fully instrumented. Figure 14 shows momentum *vs.* angle correlations of $E_\gamma = 1.8$ GeV events, conditioned on the kaon being detected in the scintillators and the pion and proton being detected in Region 1 only. This figure is to be compared with Figure 10. Predictably, events are lost at small angles and low momenta. Some fraction are also lost due to kaon and pion decay. Not included was an estimate of the reconstruction efficiency for these events.

Figure 15 shows the distribution of detected kaons in the center-of-mass frame when the above acceptance cuts are included. The differential cross sections and polarizations will be displayed as a function of kaon c.m angle, thus it is useful to examine the range of angles accessible. The upper histogram shows the flat distribution of events in the kaon c.m. angle generated by Monte Carlo, and the lower histogram shows the distribution of events which were detected. It can be seen that the distribution is fairly smooth, which encourages us to think that Monte Carlo acceptance corrections will be tractable.

Some important considerations are not included in the scope of FASTMC Monte Carlo studies. The necessary goodness of track reconstruction can not be addressed, which is related to the questions of overall efficiency and vertex resolution. Since the target will be an extended one, adequate vertex resolution is very important to all parts of the measurement program. Track reconstruction efficiency also cannot be addressed.

Figure 16 shows a typical event for $p(\gamma,K^+\pi^-p)$ as visualized using the GEANT code as implemented for the CLAS. It corresponds to a photon energy of 1.8 GeV.

5) Particle Identification and Triggering

The ratio of the production rate of hyperon events which decay into three charged particles to all events with three charged particles is about 1:130. Thus it is crucial that the on-line trigger include a "strangeness production tag". In the measurements discussed here this means that the K^+ or Λ must be identified before events are fully read-out or written to tape.

One solution is to exploit the two-body nature of the production process, which tells us that for a given photon energy there will be a one-to-one mapping between kaon angle and kaon momentum for a given recoiling mass (the Λ or Σ). For a given E_γ and recoil mass, the distribution in angle of kaons is mapped one-to-one onto the position at which the kaon is detected in the trigger hodoscope. Furthermore, since kaons reaching a particular hodoscope position have a defined momentum, their time-of-flight through the detector will also be well defined. We will use, therefore, a trigger system which can correlate, probably by means of trigger processors containing look-up tables, the photon energy (measured by a hit in the photon tagger), position of a hit on the trigger hodoscope, the particle time-of-flight, and the expected trajectory track in the drift chambers. A hierarchy of triggers will be needed to allow for differing collection and processing times of the information. Correlating hodoscope position and time-of-flight might be a first step, but there will be some particles at other momenta and on other trajectories which will have the same time-of-flight. Subsequent correlation of the actual particle trajectory with a predicted kaon trajectory then further reduces the number of non-kaons accepted by the trigger.

This method works well as long as the kaons and pions can be separated by time of flight. For the CLAS, this is true up to momenta of about 1.2 GeV/c. Figure 17 illustrates the relative numbers of pions, kaons, and protons that are to be expected from reactions induced by 1.8 GeV photons, as predicted by the CELEG event generator through the use of the LUND Monte Carlo program. The total hadronic event rate is not very energy dependent. The total cross section for $\gamma + p$ going to one nucleon plus at least one charged pion is about 200μb. The expected raw trig-

ger rate might be about 1200 Hz if we trigger on just one charged particle, while the rate of kaon production is about 6 Hz. The events in the figure correspond to a trigger requiring at least two positively charged particles in the CLAS, most of which are due to the decay of non-strange baryon resonances. For example, one source of difficulty is expected to be the reaction $\gamma + p \rightarrow \Delta^o + \pi^+$ followed by $\Delta^o \rightarrow \pi^- + p$; the Δ^o resonance is broad enough to significantly overlap the Λ and Σ mass region. The pions and kaons appear separable up to about 1.2 GeV, though the present version of FASTMC does not include all possible smearing effects which may degrade the resolution. It will probably be necessary to have a trigger counter near the target to provide a time-of-flight start signal in order to keep the coincidence window small, and hence the accidental rate low. For higher momenta a different method is needed.

Another key way of detecting strangeness photoproduction is to select those events containing a charged "V" from the decay of a neutral particle with a vertex separated from the primary interaction point. Such a topology generally comes from the decay of a neutral strange particle, since strong and electromagnetic decaying particles (Δ^o, π^o,$\Lambda(1405)$, etc.) will decay at the primary vertex. A major part of the off-line analysis will consist of finding and fitting these "V"s, first by finding hits in the chambers which combine to form tracks, then combining these tracks, using the constraints of momentum and energy conservation, to get the best description of the event in terms of kinematic variables. To the extent that this signature of strangeness production is needed in the on-line situation, there are two ways to proceed:

1) On-line track finding and fitting good enough to do rough "V"-fitting and applying a vertex cut. This cut would reject events where the decay vertex is within the detector's resolving distance of the track of the outgoing kaon. The vertex resolution of the apparatus must therefore be on the order of a few millimeters in each coordinate. This method is limited only by the computer power available at the time of the experiment.

2) Surrounding a segmented target with a thin multiplicity hodoscope and doing an on-line multiplicity count: trigger on events with one charged particle leaving the target (the kaon) and at least two charged particles at the external trigger hodoscope (the kaon plus the decay pion or proton). This method is straightforward electronically, but construction of the required target would be technically difficult, since the target is long and most of the Λ's go into a forward cone. It would require a segmented cryogenic target closely surrounded by many channels of fine-grained detectors and readout.

The most direct way to detect strangeness photoproduction is to reconstruct the invariant or missing mass of the strange particles produced. Figure 18 shows the Λ missing mass reconstructed from the gamma-K arms of the data using FASTMC for the resolution function (partly

modified for the case of 20% of the full magnetic field). The FWHM resolution is 8.5 MeV. In this figure only "good" kaon events are used. If a high momentum pion is mistaken for a kaon, the reconstructed gamma-K missing mass is much worse, as seen in Figure 19. A cut on this spectrum will reject a large fraction of the pions not rejected by time of flight. Next, if three final state particles are detected, full kinematic reconstruction will always reveal whether a given event fits the Λ or Σ production hypothesis or not.

The most likely trigger scenario for these measurements is to require one particle in the scintillators at the first level of the trigger, and hits for at least two more tracks in the inner drift chambers at a higher trigger level. Correlation of angle (CLAS hodoscope element) and photon energy (tagger element) will reject many pion events, and this can be done without track reconstruction calculations. After the track angle is known, K/π separation by time of flight will be used to reduce the number of pions in the trigger, as discussed above. Subsequently, more time consuming missing mass or vertex reconstruction calculations can be done.

Run Plan and Beam Time Estimate

In the first round of experimentation using the CLAS we intend to measure Λ and Σ^o photoproduction from threshold up to the limit of K/π time-of-flight separation, or from $E_\gamma = .911$ GeV to $E_\gamma = 1.8$ GeV. The main goal is to measure the Λ and Σ^o differential cross sections and polarizations using the self-analyzing decay of the Λ as a "polarimeter". In addition, we request some time for exploratory measurements at higher beam energies for detecting the production of Y^* resonances and for electroproduction tests.

Beam energy = 2.0 GeV
Tagging range = 0.90 to 1.80 GeV
Photon Energy Resolution = 5 MeV
Photon Energy Bin Width = 50MeV (average) with closer spacing closer to threshold
Number of Photon Energy Bins = 18
Tagging Rate = 10 MHz overall, 5×10^5 per bin, with higher rates at lower energies
(a la bremsstrahlung yield)
Rate of detectable (K,π^-,p) events = 4/sec over whole photon energy range
= 14,400/hour
= 0.2/sec per energy bin

Each energy bin will be divided into 10 angle bins. In each angle bin we want to measure a polarization of the Λ which is in the neighborhood of 0.3. Measuring such a polarization to ±0.05 accuracy requires about 950 decays. Hence we need

(950 events/energy bin/angle bin)(10 angle bins)/(0.2 events/sec)
$= 4.7\times10^4$ seconds = <u>13.2 hours</u>.

The average class acceptance is 5% for these events, and we estimate that the event reconstruction efficiency will be perhaps 50%. Then we need

(13.2 hours)/(0.05)/(0.5) = <u>528 hours</u>.

Time for exploratory measurements: <u>100 hours</u>.
With 72 hours of setup time we arrive at

528 + 100 + 72 = <u>700 hours</u>. (Beam time request)

Figure 20 shows the expected statistical precision we may obtain with the above beam time for the polarization of the Λ, in comparison to the existing data. We note also that these measurements should be compatible with simultaneous running of several other photoproduction experiments.

Resources Required

A summary of the resources needed for measurements of strangeness photoproduction at CEBAF is:

1) The CLAS detector: a detector system capable of tracking several particles from the reactions discussed over a large angular range. Forward angle coverage (below about 60^o) is most important but close to 4π coverage is needed since at least one particle can always go backward. Mass resolution in the (γ,K) arm must be sufficient to separate Λ from Σ^o production.

2) Photon tagger. A broad banded tagged photon beam with 5 to 10 MeV resolution is most suitable. The highest possible rates ($\approx 10^7$ tagged photons/sec) are needed.

3) Liquid hydrogen target. This must be of a design suited to a large acceptance device, with thin walls on all sides and a minimum of external "plumbing".

4) Strangeness Production Identification System. Crucial to a successful program is the development of a trigger system with trigger processors capable of selecting strange particle production events. Elements of this system are: 1) exploiting the two-body kinematics of the strangeness production reaction to select kaons (angle/time-of-flight correlations); 2) selecting hyperon events by reconstructing the strange decay vertex, which is spatially separated from the kaon ray; 3) rejecting pionic events such as from Δ^o production by reconstructing the Λ missing mass from γ,K; 4) rejecting pionic events by reconstructing the Λ invariant mass from the final state decay pion and proton.

Manpower Commitments

The individuals listed on this proposal are either directly involved in the development of this measurement program, or have extensive experience in areas of high energy physics that will eventually benefit the collaboration. There is direct theory support at VPI. The photon tagger, which is necessary for these measurements, is being developed by the group members from Catholic University. Carnegie Mellon is participating in the development of the Region 1 drift chambers for the CLAS, while Florida State is involved in the general software development effort.

References

1] See for example: R. Schwarz *et al.*, AIP Conf. Proc. **95** "High Energy Spin Physics," G. Bunce, Ed., (1982) 114.

2] P.D.Barnes *et al.* Phys Lett. B **189** (1987) 249.

3] K. Heller, AIP Conf. Proc. **95** "High Energy Spin Physics," G. Bunce, Ed., (1982) 320, and references therein.

4] See for example: C.J.Bebek *et al*, Phys Rev Lett. **74** (1974) 21.

5] Earliest published measurements: P.L.Donoho and R.L.Walker, Phys. Rev. **107** (1957) 1198; A. Silverman, R.R.Wilson, and W. M. Woodward, Phys. Rev 108 (1957) 501; P.L.Donoho and R.L.Walker, Phys. Rev **112** (1958) 981; B. D. McDaniel, A. Silverman, R.R.Wilson, and G. Cortellessa, Phys. Rev. **115** (1959) 1039. Earliest Λ polarization measurements: H. Thom, E. Gabathuler, D. Jones, B.D.McDaniel, and W.M.Woodward, Phys Rev. Lett. **11** (1963) 433.

6] Available data are summarized in R.A.Adelseck, C. Bennhold, and L.E.Wright, Phys. Rev. **C32** (1985) 1681.

7] Y.Renard Nucl. Phys. **B40** (1972) 499; F. M. Renard and Y. Renard, Nucl. Phys. **B25** (1971) 491.

8] T. Fujii *et al.*, Phys. Rev. D **2** (1970) 439.

9] M. Kohno and W. Weise, Phys Lett. B **179** (1986) 15.

10] T.K.Kuo, Phys. Rev. **129** (1963) 2264.

11] H. Thom, Phys. Rev. **151** (1966) 1322.

12] A. R. Pickering, Nucl. Phys. **B66** (1973) 493.

13] A. S. Rosenthal, Dean Halderson, Kimberly Hodgkinson, and Frank Tabakin, Annals of Physics **184** (1988) 33.

15] Ya. I. Granovskii and V.N. Starikov, Sov. J. Nucl. Phys. **6** (1968) 444.

16] Carl B. Dover and George E. Walker, Phys. Rep. **89** (1982) 1.

17] O. Dumbrajs et al., Nucl. Phys. **B216** (1983) 277.

18] M. Bozoian, J.C.H. van Doremalen, and H.J.Weber, Phys. Lett **122B** (1983) 637.

19] C.P.Knudsen and E. Pietarinen, Nucl. Phys. **B57** (1973) 637.

20] R.A.Adelseck and L.E.Wright, Phys. Rev. **C38** (1988) 1965; Ralf Anton Adelseck, PhD thesis, Ohio University (1988).

21] H. Tanabe, M. Kohno, and C. Bennhold, Contribution to 1988 CEBAF Summer Workshop; and Mainz Preprint, 1988.

22] R.L.Workman, Phys Rev **C39** (1989) 2076; reply to comment by Workman in R.A.Adelseck and L.E.Wright, Phys Rev **C39** (1989) 2078.

23] R.L. Workman, Contribution to "Few Body XII"

24] Joseph Cohen, Phys. Lett. B **192** (1987) 291; Joseph Cohen, Phys. Rev. C **37** (1988) 187.

25] R.A. Adelseck and B. Saghai, "10eme session d'etudes biennale de Physique Nucleaire", Aussois, France, 1989.
26] R.L.Workman, "Observables in kaon Photoproduction" (unpublished)
27] K.H.Althoff *et al,* Nucl. Phys. **B137** (1978) 269.
28] C. Bennhold and L.Wright, to be published.
29] P. Feller, D. Menze, U. Opara, W. Schulz, and W.J.Schwille, Nucl. Phys. **B39** (1972) 413.
30] Harry J. Lipkin, Phys. Rep. **8C** (1973) 175.
31] C. Bennhold, "The Electromagnetic Production of Σ-hypernuclei" (preprint)
32] "The CEBAF Tagged Photon Beam" Daniel I. Sober *et al,* CEBAF End Station B PCDR, Appendix R, 1989.
33] Elton Smith, FASTMC CLAS-NOTE-89-003.
34] Don Joyce, CELEG Monte Carlo, CEBAF.

Table I

Values of $g_{K\Lambda N}/\sqrt{4\pi}$ obtained by various authors. Adapted from Ref 20] and Ref 23].

	$\frac{g_{K\Lambda N}}{\sqrt{4\pi}}$	Reference
From analysis of photoproduction data:		
Kuo '63	2.0	10
Thom '66	2.49	11
Renard '71	1.1 to 2.8	7
Pickering '73	2.8 to 3.4	12
Adelseck, Bennhold, and Wright '85	1.03±.12	6
Rosenthal *et al* '88	0.92	13
Adelseck and Wright '88	4.3	20
Workman '89	3.13±1.02	30
From analysis of hadronic data:		
Granovskii and Starikov '68	2.43	15
Dover and Walker '83	4.62	16
Dumbrajs '83	3.73	17
Bozoian et al '83	4.13	18
Knudsen and Pietarinen '73	3.5±2.5	19

Figure Captions

Figure 1) Quark flow diagrams for strangeness production in three different reactions. Real and/or virtual strangeness photoproduction can be studied at CEBAF.

Figure 2) Overview of the existing strangeness photoproduction differential cross sections for $p(\gamma,K^+)\Lambda$ from Renard (Ref 7]). Differential cross sections for K^+ production are plotted as a function of kaon c.m. angle. The shaded region corresponds to $g_{\Lambda KN}/\sqrt{4\pi}$ varying from 1.1 to 2.8.

Figure 3) (a)(b) Overview of the Λ polarization data for $p(\gamma,K^+)\Lambda$ for a kaon c.m. angle of $90^o \pm 5^o$. (a) From Renard (Ref. 7]), with curves corresponding to those in Figure 2. Note the sensitivity of this model to the polarization data. (b) From a newer compilation and calculation by Adelseck (Ref 20]). Polarization has opposite sign definition from (a). (c) Λ polarization data at a function of angle for several energies, from Ref. 8] (d) Prediction from Ref 20] of the angular distribution of the Λ polarization as a function of kaon c.m. angle at 1.2 GeV.

Figure 4) Born diagrams used in calculations of strangeness photoproduction (From Ref.20]).

Figure 5) Total $\gamma p \rightarrow K^+ \Lambda$ cross section with several calculations, including those of Tanabe, Kohno, and Bennhold [21] (solid line).

Figure 6) Prediction from Ref. 25] of three polarization variables using several models which all describe the differential cross section well. See text for explanation.

Figure 7) Predictions from Ref. 28] for the reaction $^{16}O(\gamma,K^+)^{16}_{\Lambda}N$, using several models for the elementary photoproduction operator. The models are: solid line, Ref 20]; dashed line, Ref 6]; dot-dashed line, Ref 11].

Figure 8) Overview of existing Σ^o photoproduction data [7].

Figure 9) Three body-phase space for strangeness photoproduction in $\gamma + p \rightarrow K^+ + \Lambda$ for $E\gamma =$ 1.1 GeV. Note the strong forward peaking of all detected particles. No acceptance cuts have been applied.

Figure 10) Three body-phase space for strangeness photoproduction in $\gamma + p \rightarrow K^+ + \Lambda$ for $E\gamma =$ 1.8 GeV. No acceptance cuts have been applied.

Figure 11) Acceptance of the CLAS using FASTMC for triggering on K^+,π^-,p final states resulting from $p(\gamma,K^+)\Lambda$. Nominal magnetic field strength was specified and positive particles bend inward. For all curves, the kaons were detected in the scintillators. Upper, middle, and lower curves correspond to the $\pi^-$and p reaching Region 1, Region 2, and the scintillators, respectively. Thus the geometrical and momentum acceptances, and also the decay probabilities of the K and π are included in these curves. The event reconstruction efficiency is not included.

Figure 12) Acceptance of the CLAS for triggering on K^+,π^-,p final states using FASTMC with one fifth of the nominal magnetic field strength was specified. The rest is as for the previous figure.

Figure 13) Acceptance of the CLAS for triggering on K^+,p final states using FASTMC with one fifth of the nominal magnetic field strength was specified and positive particles bend outward. There is no detectable acceptance increase when the proton is not required to travel as far as the scintillators.

Figure 14) Three body-phase space for strangeness photoproduction in $\gamma + p \rightarrow K^+ + \Lambda$ for $E_\gamma =$ 1.8 GeV. Acceptance cuts are that kaons must reach scintillators, while pion and proton reach Region 1.

Figure 15) Kaon center-of-mass angular distribution for the geometrical and particle energy acceptances expected for the CLAS detector. The upper histogram shows the events generated by Monte Carlo, while the lower histogram shows the events accepted.

Figure 16) An event simulated using GEANT, for $E\gamma$=1.8 GeV.

Figure 17) Time of flight (per meter) vs. momentum for pions, kaons, and protons detected in the CLAS. The relative particle densities correspond to all the hadronic final states induced by 1.8 GeV photons.

Figure 18) Invariant mass of lambda using photon and kaon, for $E\gamma = 1.8$ GeV, $\Delta E_\gamma = 5$ MeV, one fifth of nominal magnetic field, and no vertex information assumed (Using FASTMC). FWHM = 8.5 MeV.

Figure 19) Invariant mass of "lambda" using photon and kaon, as in previous figure, but with a pion misidentified as a kaon. Pion comes from Δ decay. Note the change in horizontal scale.

Figure 20) Λ polarization data at a function of angle for several energies, from Ref. 8], together with estimated errors of new data gathered with the CLAS at CEBAF.

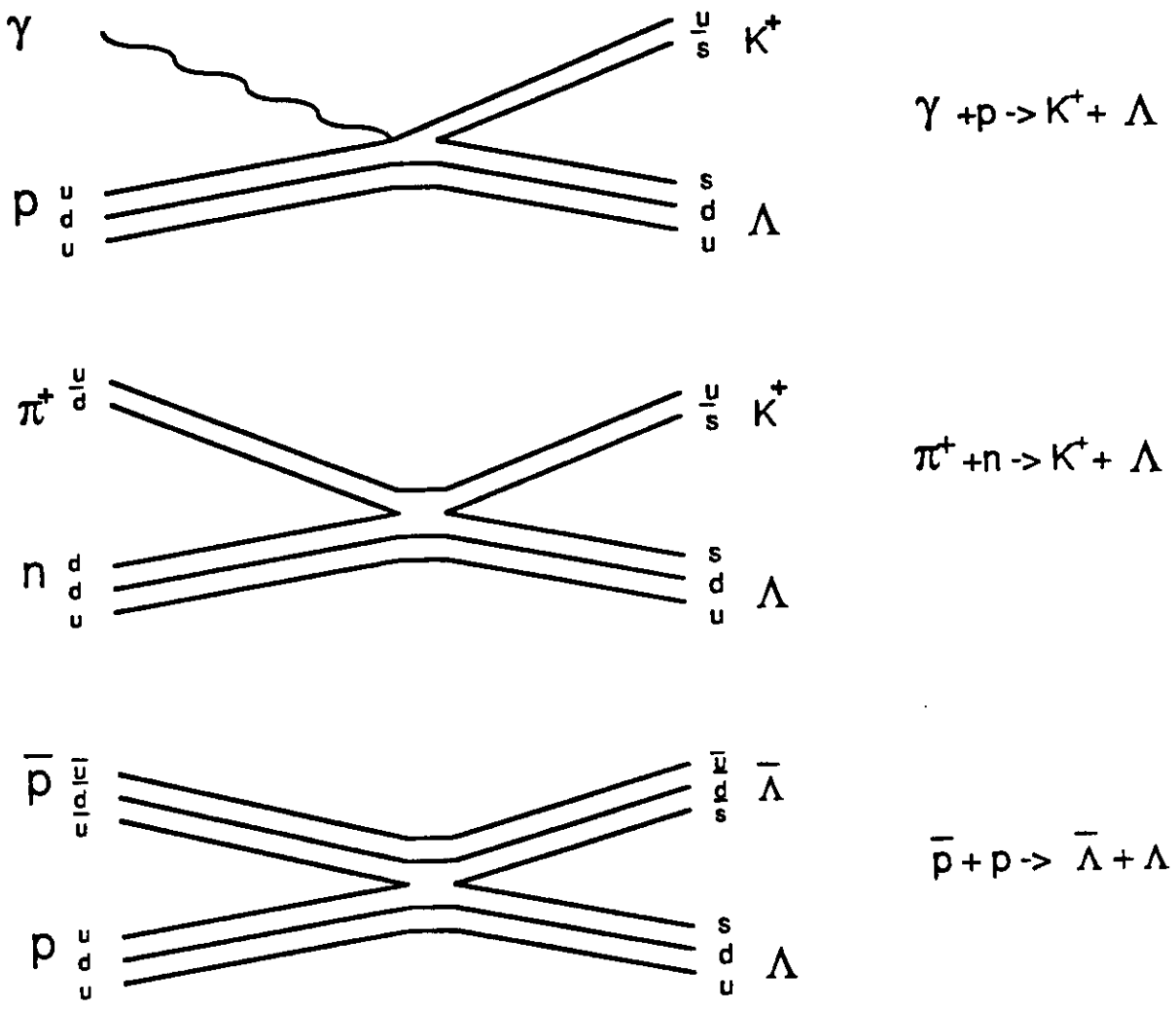
γ
p
u d u
u s
K+
s d u
Λ
γ +p -> K+ + Λ
π+
d u
n
u d d
u s
K+
s d u
Λ
π+ +n -> K+ + Λ
p̄
ū ū d̄
d̄ s̄
Λ̄
p
u d u
s d u
Λ
p̄ + p -> Λ̄ + Λ

Figure 1

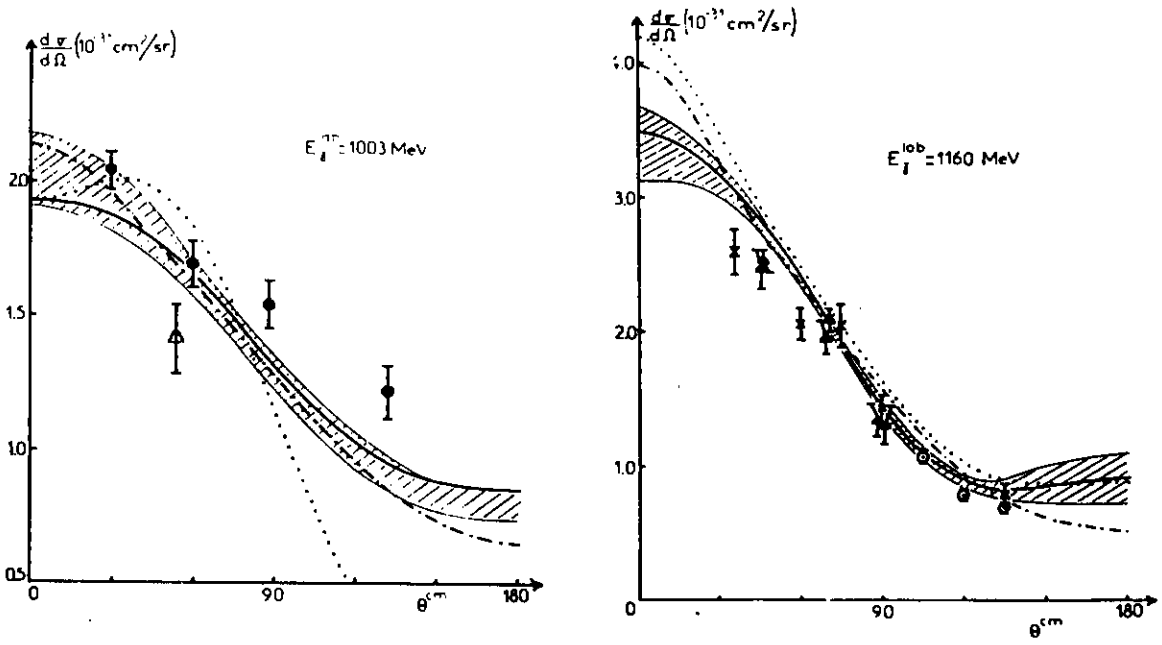
$\frac{d\sigma}{d\Omega}$ (10^{-31} cm^2/sr)
E_γ^{lab} = 1003 MeV
2.0
1.5
1.0
0.5
0
90
θ^{cm}
180
$\frac{d\sigma}{d\Omega}$ (10^{-31} cm^2/sr)
E_γ^{lab} = 1160 MeV
3.0
2.0
1.0
0
90
θ^{cm}
180

Figure 2

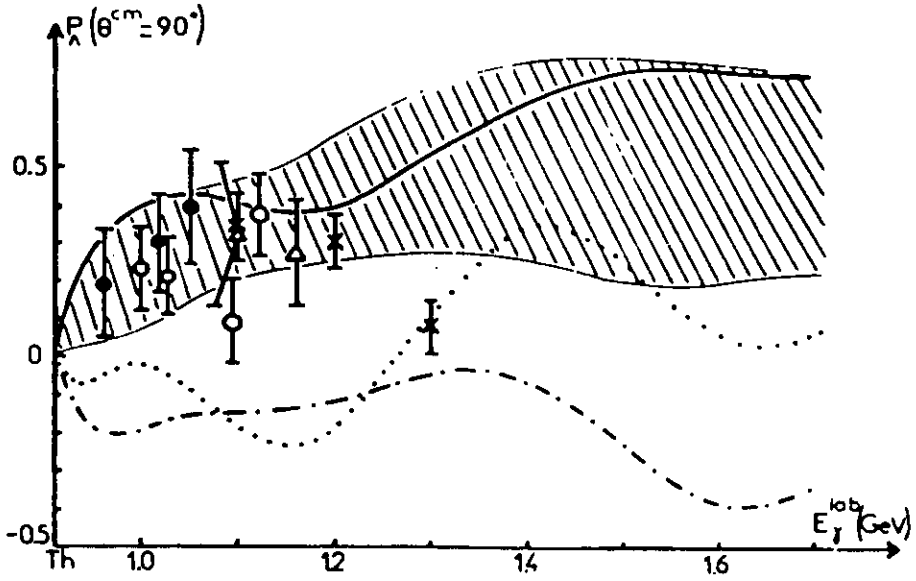
$P_\Lambda(\theta^{cm}=90^\circ)$
0.5
0
-0.5
Th
1.0
1.2
1.4
1.6
E_γ^{lab} (GeV)

a)

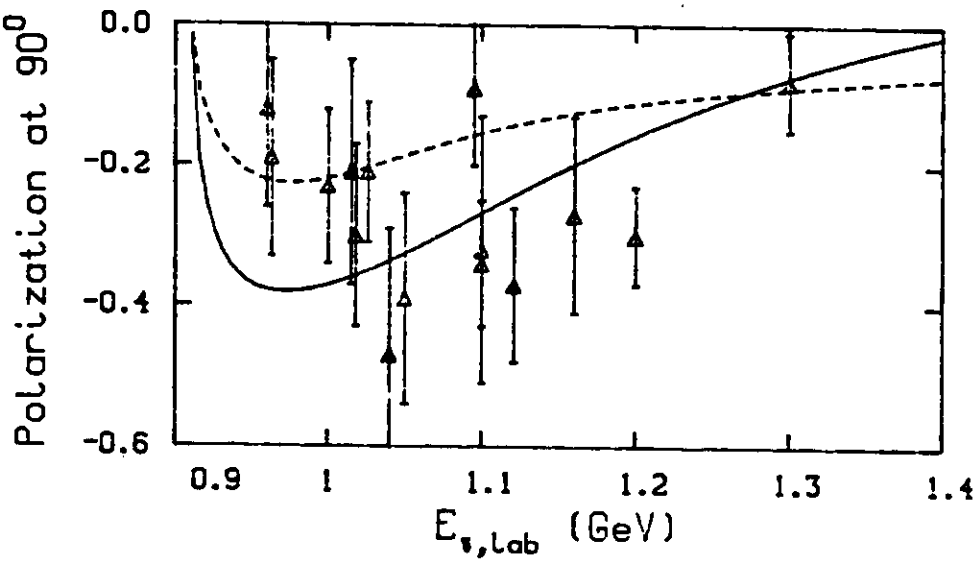
Polarization at 90°
0.0
-0.2
-0.4
-0.6
0.9
1
1.1
1.2
1.3
1.4
$E_{\gamma,Lab}$ (GeV)

b)

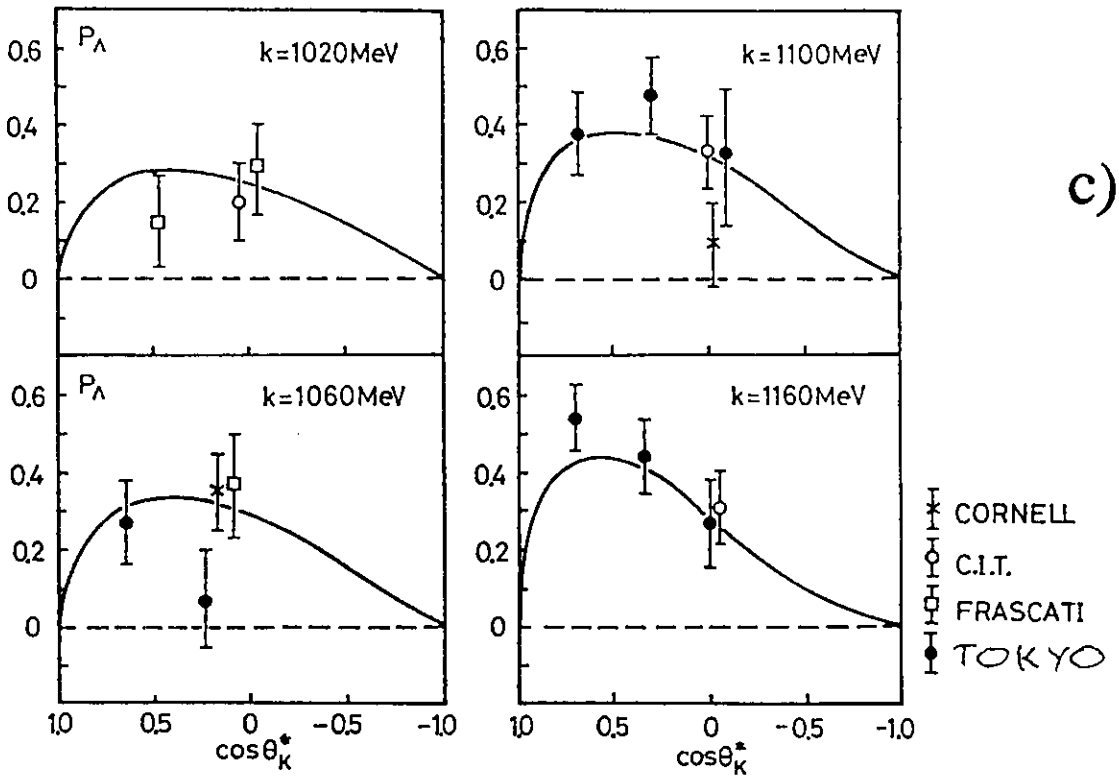
P_Λ
k=1020MeV
k=1100MeV
k=1060MeV
k=1160MeV
0.6
0.4
0.2
0
1.0
0.5
0
-0.5
-1.0
cosθ*K
CORNELL
C.I.T.
FRASCATI
TOKYO

c)

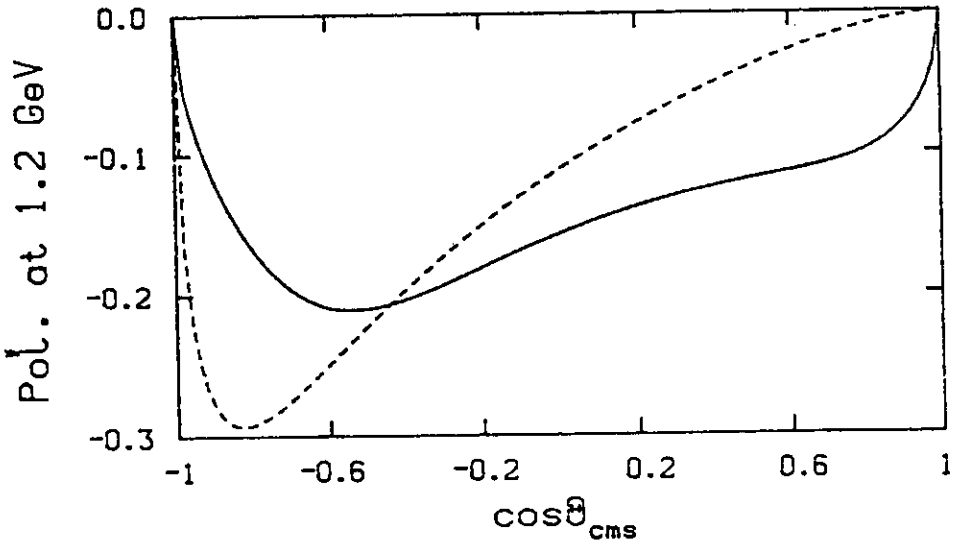
Pol. at 1.2 GeV
0.0
-0.1
-0.2
-0.3
-1
-0.6
-0.2
0.2
0.6
1
cosθcms

d)

Figure 3

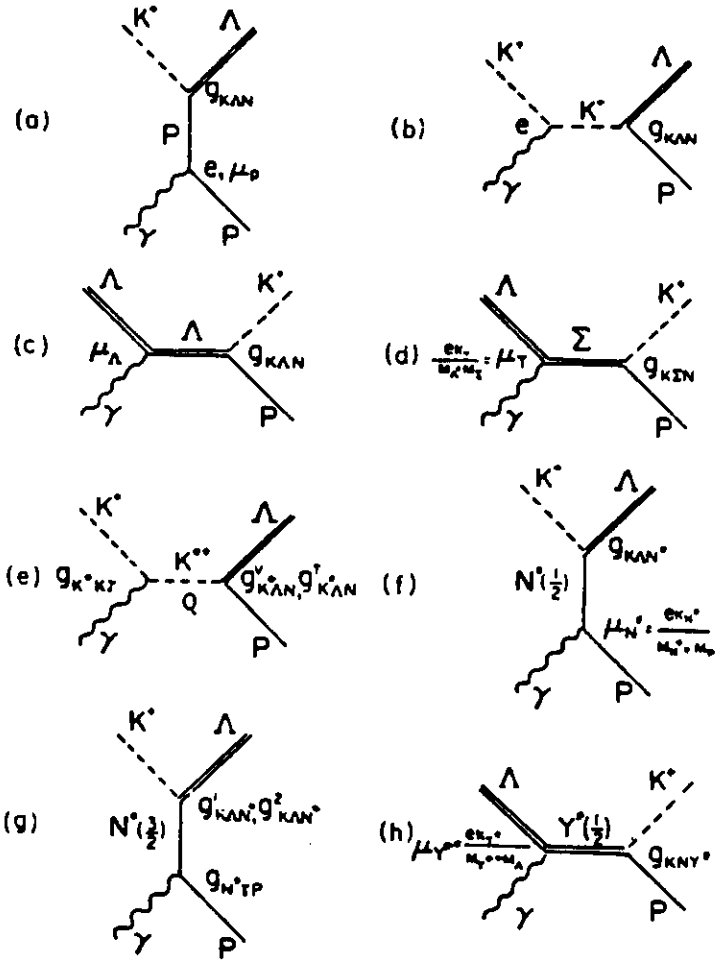

Feynman diagrams for the process $p(\gamma,K^+)\Lambda$. (a)-(c) show the Born terms, (d) stands for the Σ exchange, (e) represents the spin-1 kaon resonances, (f) and (g) represent the spin 1/2 and 3/2 nucleon resonances, and (h) stands for the spin 1/2 hyperon resonances.

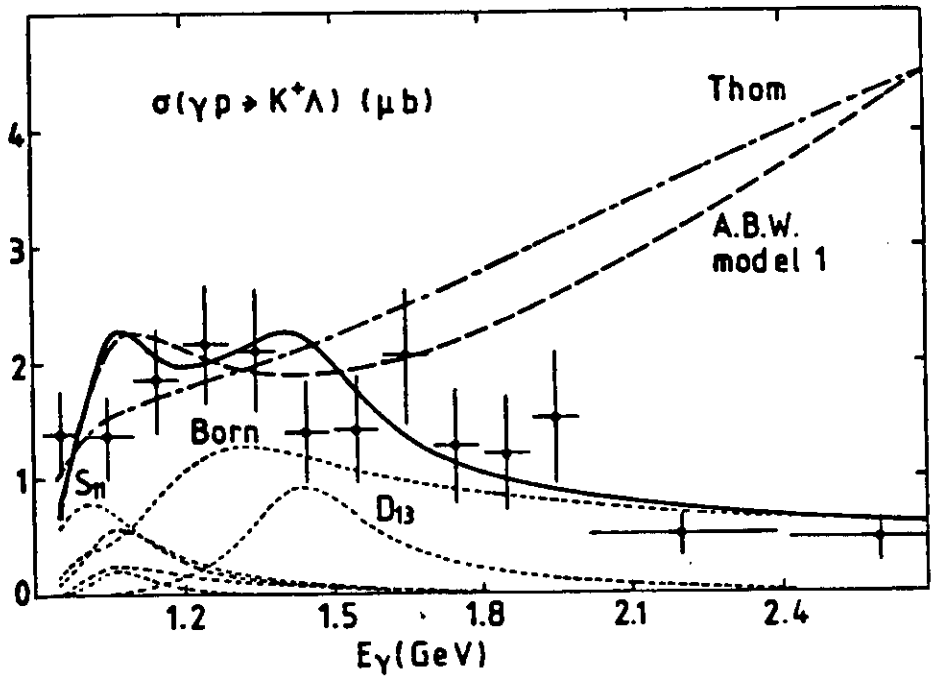

The $\gamma p \rightarrow K^+\Lambda$ total cross sections. The solid curve shows our results together with the separation of Born and resonance contributions. The dashed curve stands for the prediction of model 1 of ref. [2], and the dash-dotted curve for Thom's model [1].

Figure 5

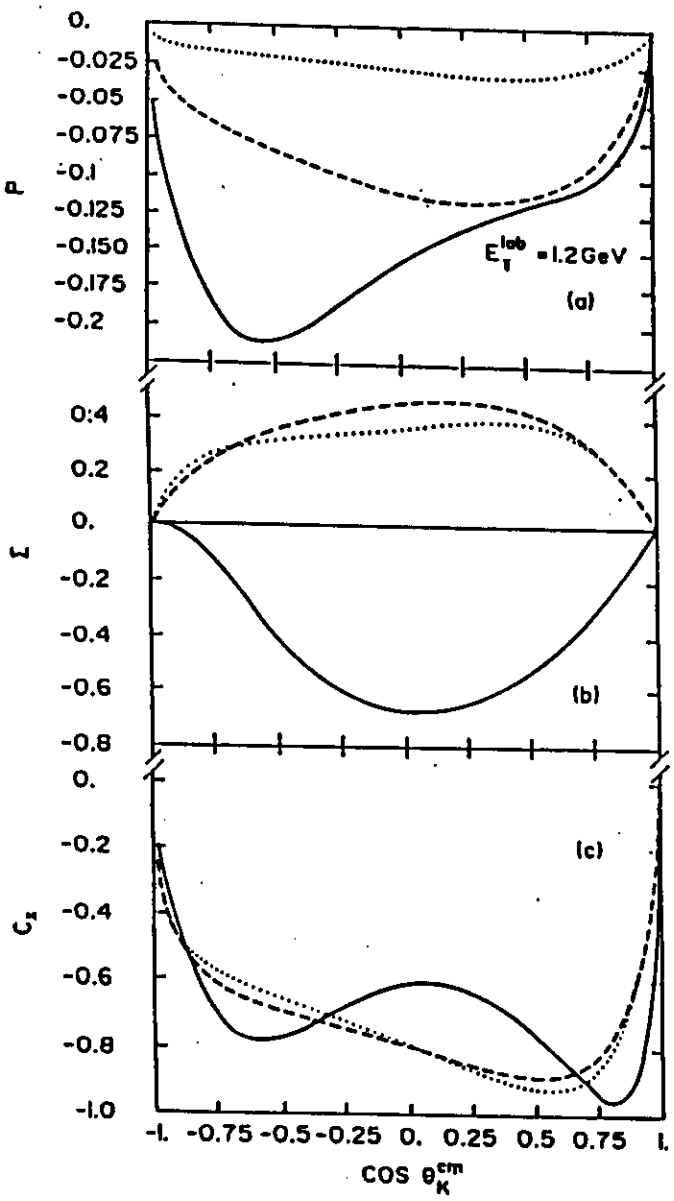

Angular distribution of the asymmetry observables P, Σ and C_x. The notation agrees with Fig. 3.

Figure 6

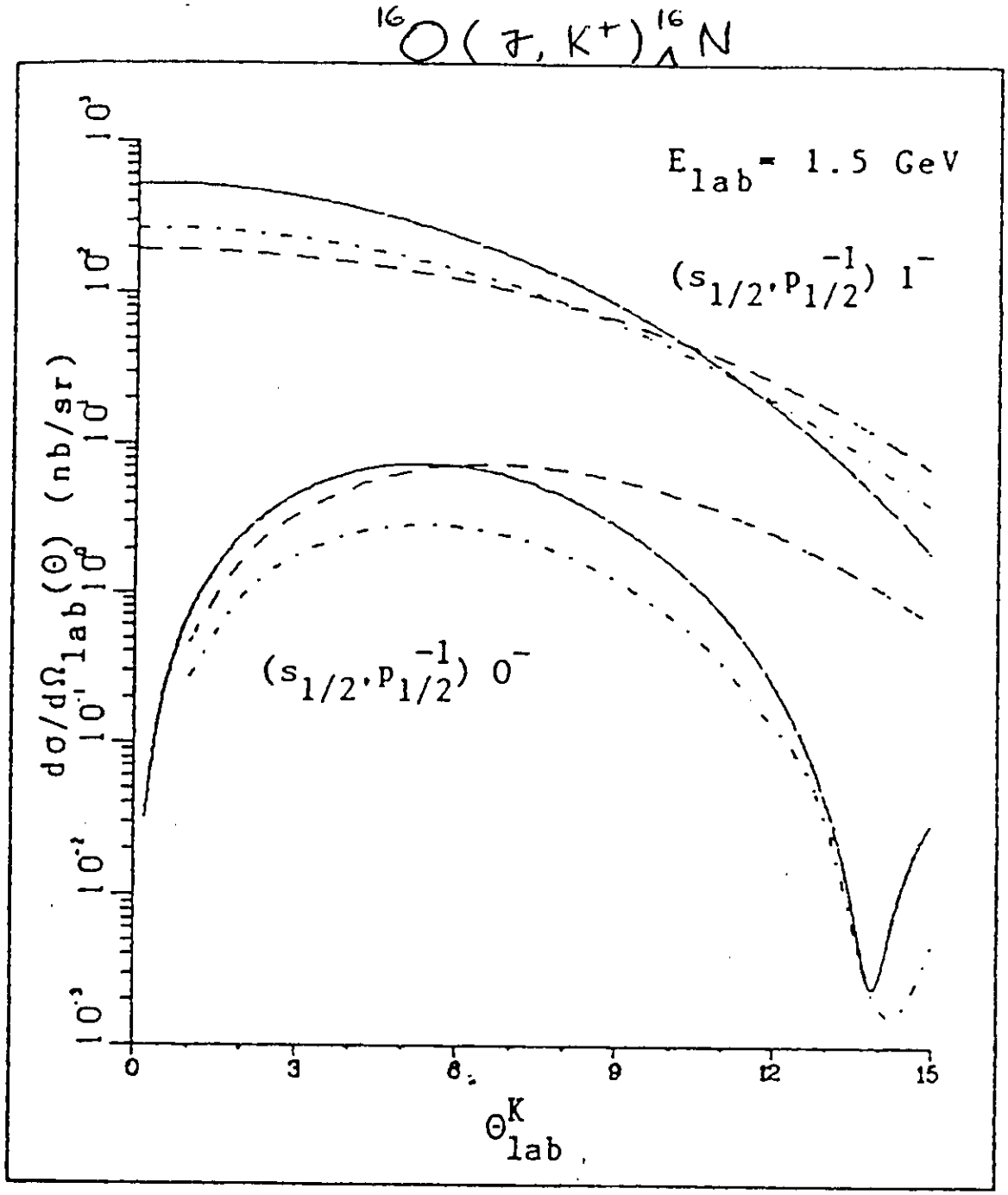
$^{16}O(\pi, K^+)^{16}_{\Lambda}N$
E_{lab} = 1.5 GeV
$(s_{1/2}, p_{1/2}^{-1})$ 1^-
$(s_{1/2}, p_{1/2}^{-1})$ 0^-
$d\sigma/d\Omega_{lab}(\Theta)$ (nb/sr)
10^3
10^2
10^1
10^0
10^{-1}
10^{-2}
0
3
6
9
12
15
Θ^K_{lab}

Figure 7

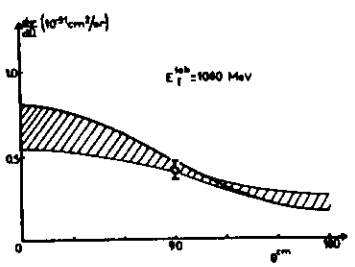

Fig. 6a.

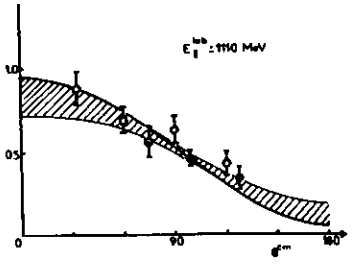

Fig. 6b.

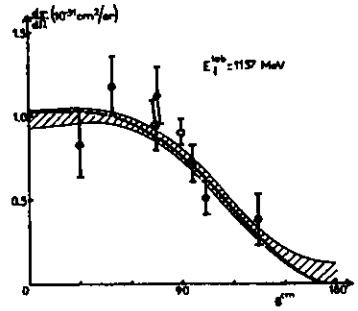

Fig. 6c.

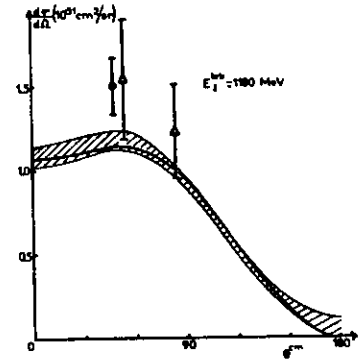

Fig. 6d.

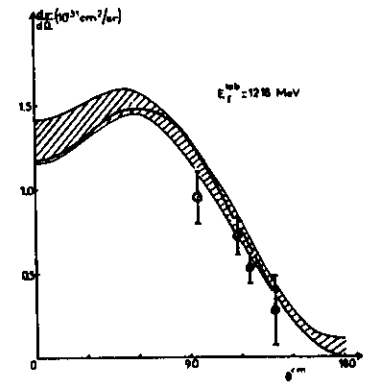

Fig. 6e.

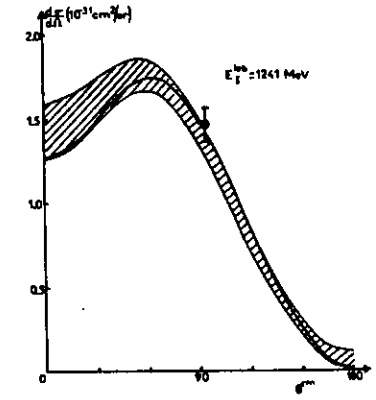

Fig. 6f.

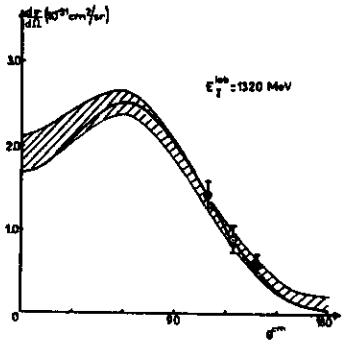

Fig. 6g.

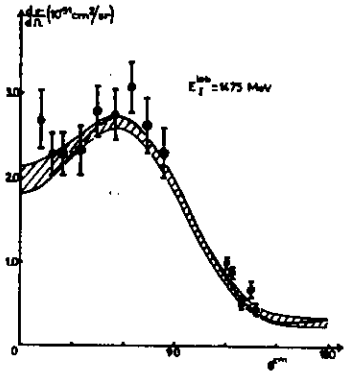

Fig. 6h.

Angular distribution for $d\sigma/d\Omega$ for the reaction $\gamma p \to K^+\Sigma^0$ at E_γ^{lab} =

(a) 1080 MeV,	(e) 1218 MeV,
(b) 1110 MeV,	(f) 1241 MeV,
(c) 1157 MeV,	(g) 1320 MeV,
(d) 1180 MeV,	(h) 1475 MeV,

The unbroken line (fit 2) has $g_{\Lambda KN} = -8.56$, $g_{\Sigma KN} = 1.95$. The hatched region indicates the range of values obtained with fits 1-4 and $-12.7 \leq g_{\Lambda KN} \leq -4$, $g_{\Sigma KN} = 1.95$. References for the experimental data are: ● R. L. Anderson et al., Phys. Rev. Letters 9 (1962) 131; ○ R. L. Anderson et al., Int. Symp. on electron and photon interactions, Hamburg (1965); ⊕ A. Bleckmann et al., preprint, Bonn Universität (1970); ⊖ B. Dudelzak et al., LAL 1236, Orsay (1970); △ T. Fujii et al., preprint, Tokyo University (1969-1970).

Figure 8

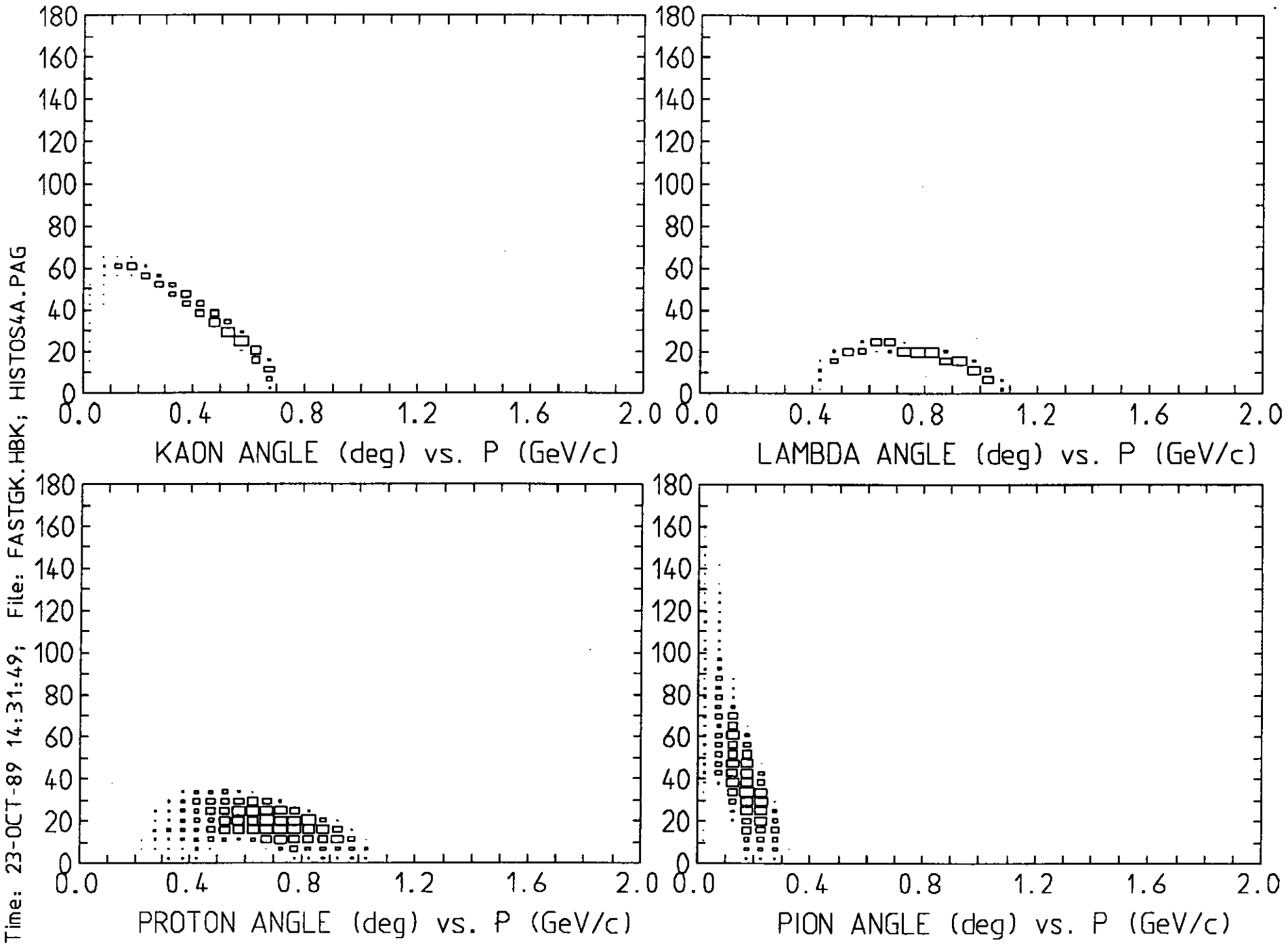
KAON ANGLE (deg) vs. P (GeV/c)
LAMBDA ANGLE (deg) vs. P (GeV/c)
PROTON ANGLE (deg) vs. P (GeV/c)
PION ANGLE (deg) vs. P (GeV/c)
Time: 23-OCT-89 14:31:49; File: FASTGK.HBK; HISTOS4A.PAG

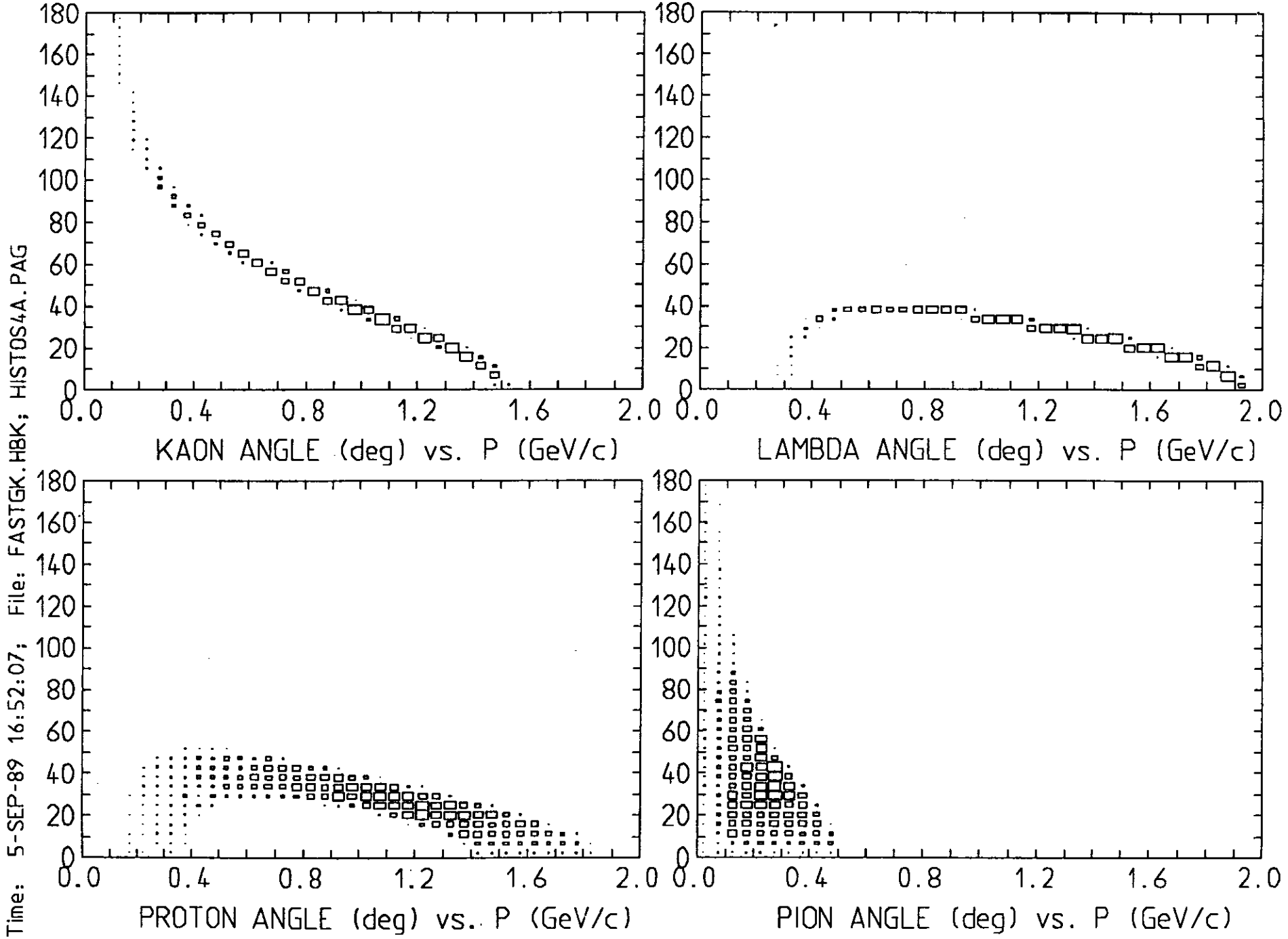
KAON ANGLE (deg) vs. P (GeV/c)
LAMBDA ANGLE (deg) vs. P (GeV/c)
PROTON ANGLE (deg) vs. P (GeV/c)
PION ANGLE (deg) vs. P (GeV/c)
Time: 5-SEP-89 16:52:07; File: FASTGK.HBK; HISTOS4A.PAG

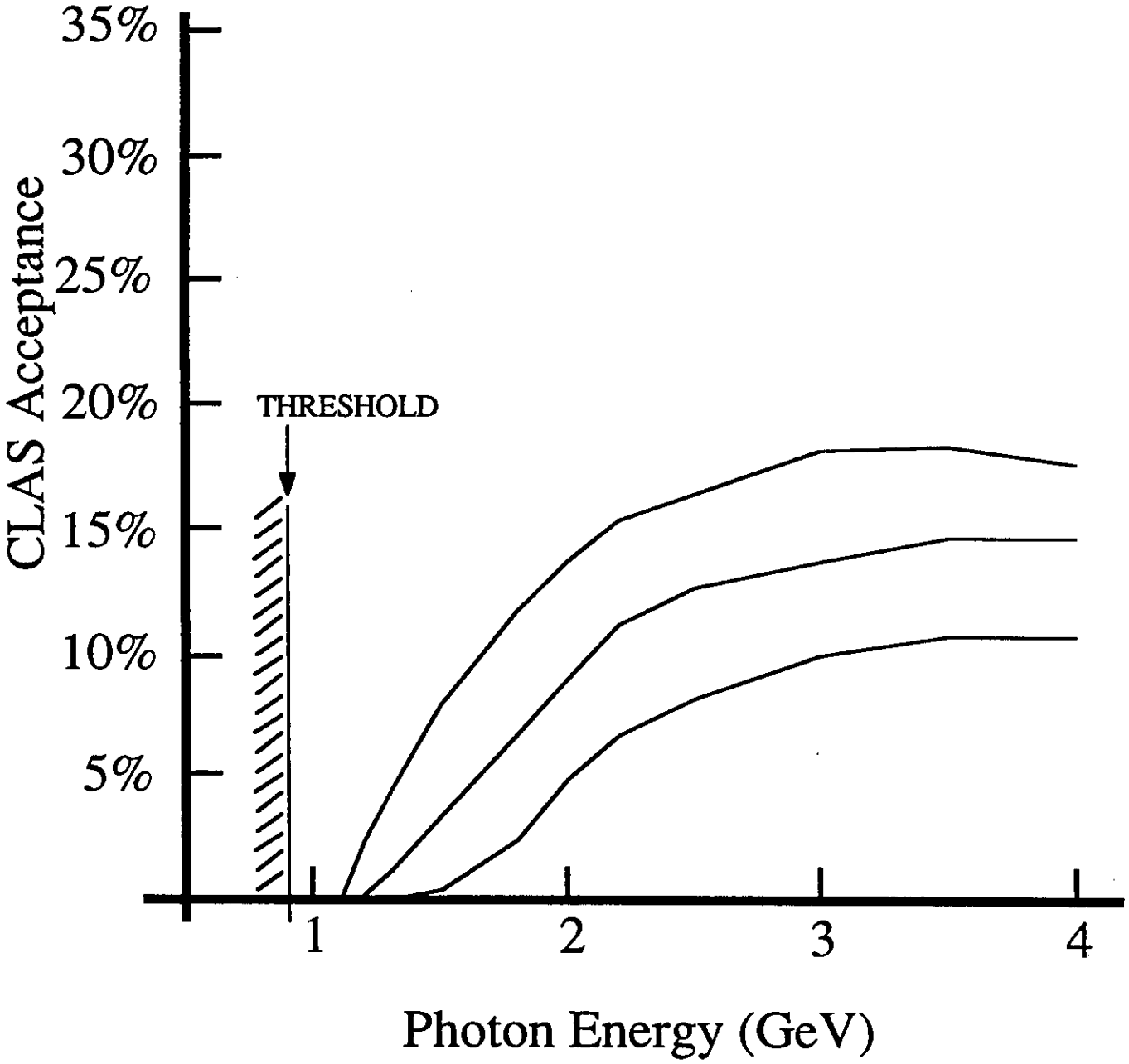

Figure 11

$p(\gamma,K^+)\Lambda$, MEASURING K^+,π^-,p FINAL STATE
FULL FIELD, POSITIVES BENDING INWARD

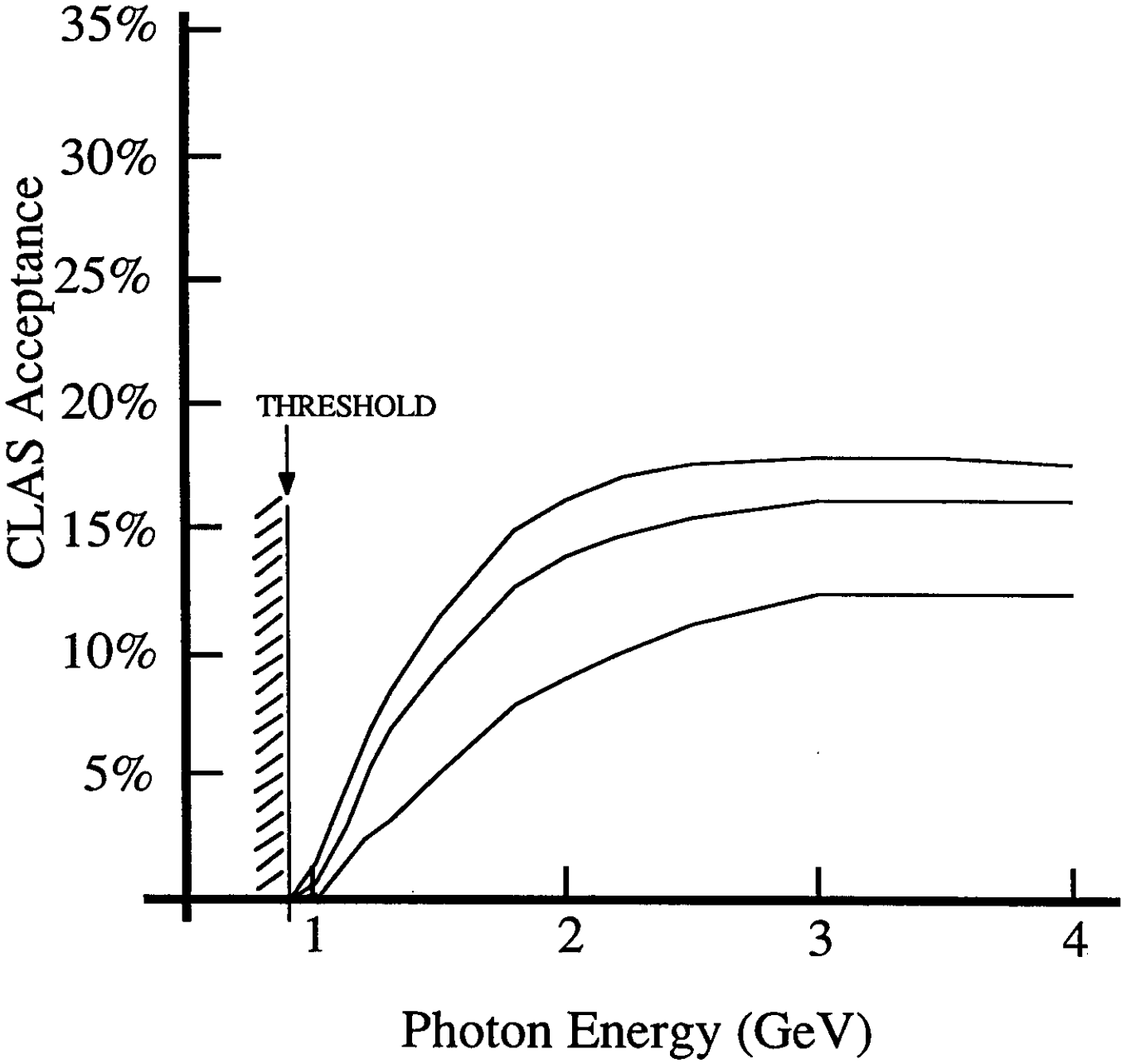

Figure 12

$p(\gamma,K^+)\Lambda$, MEASURING K^+,π^-,p FINAL STATE
0.2 FIELD, POSITIVES BENDING INWARD

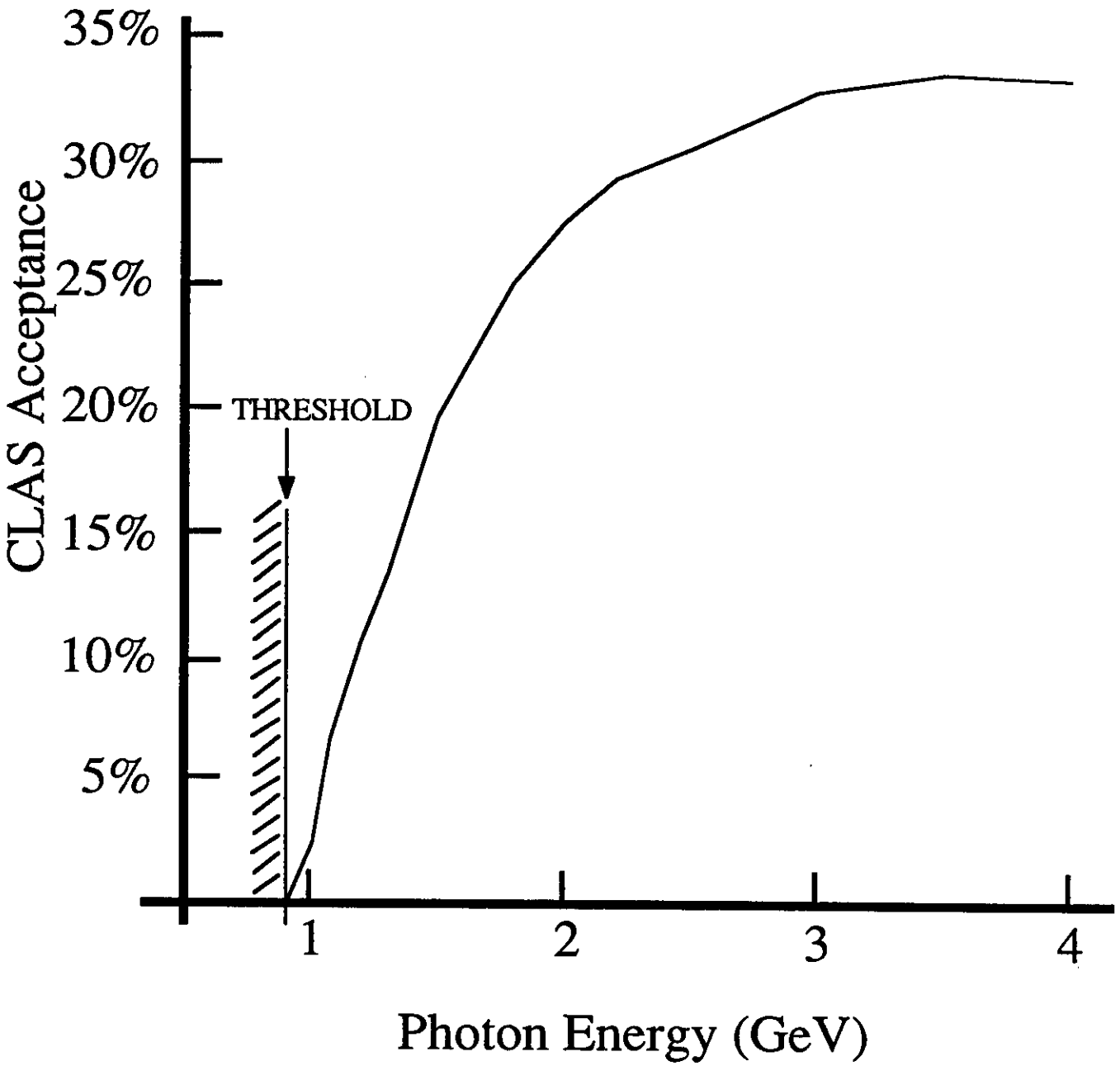

Figure 13

$p(\gamma,K^+)\Lambda$, MEASURING K^+,p FINAL STATE
0.2 FIELD, POSITIVES BENDING OUTWARD

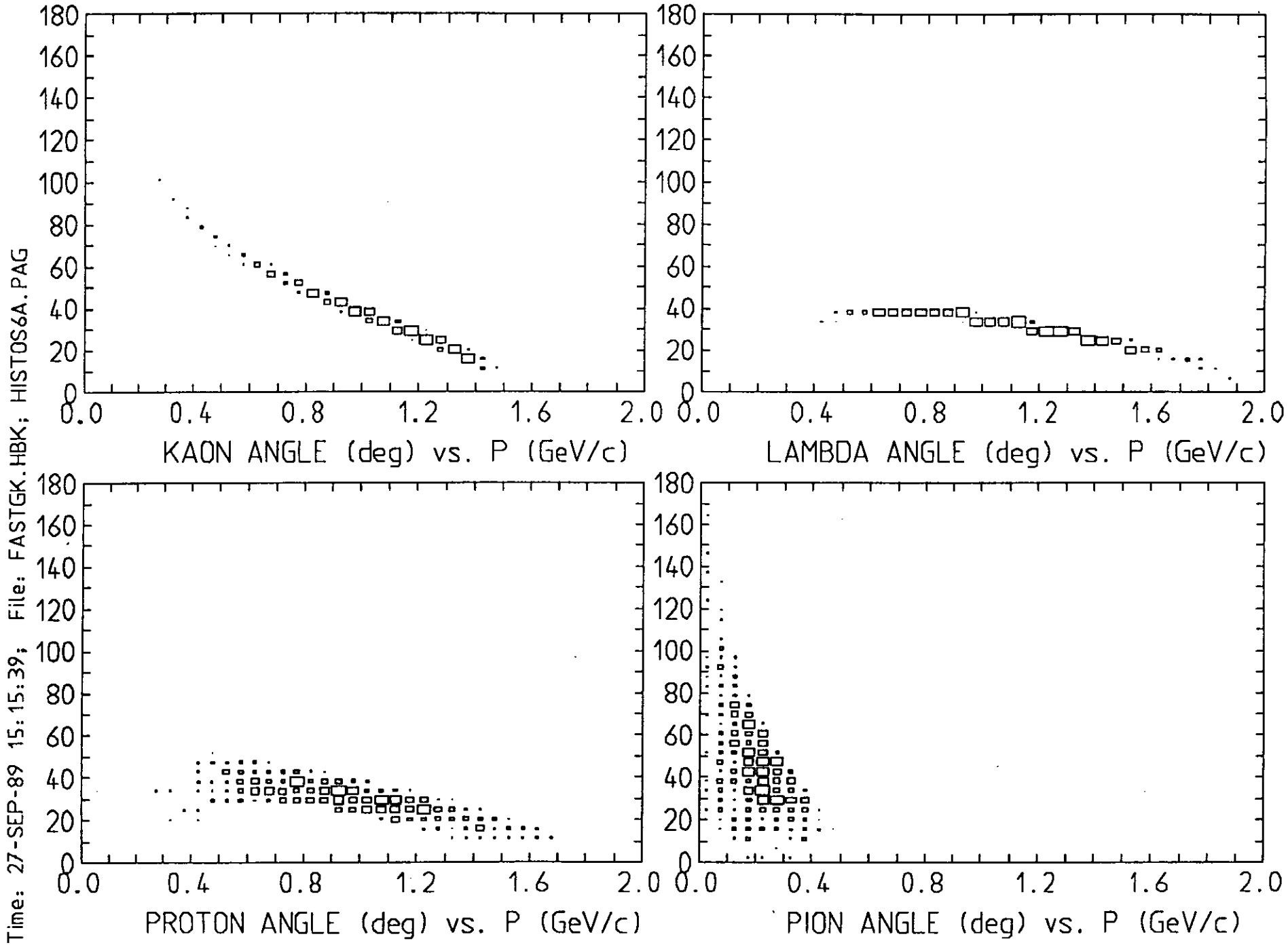
KAON ANGLE (deg) vs. P (GeV/c)
LAMBDA ANGLE (deg) vs. P (GeV/c)
PROTON ANGLE (deg) vs. P (GeV/c)
PION ANGLE (deg) vs. P (GeV/c)
Time: 27-SEP-89 15:15:39; File: FASTGK.HBK; HISTOS6A.PAG

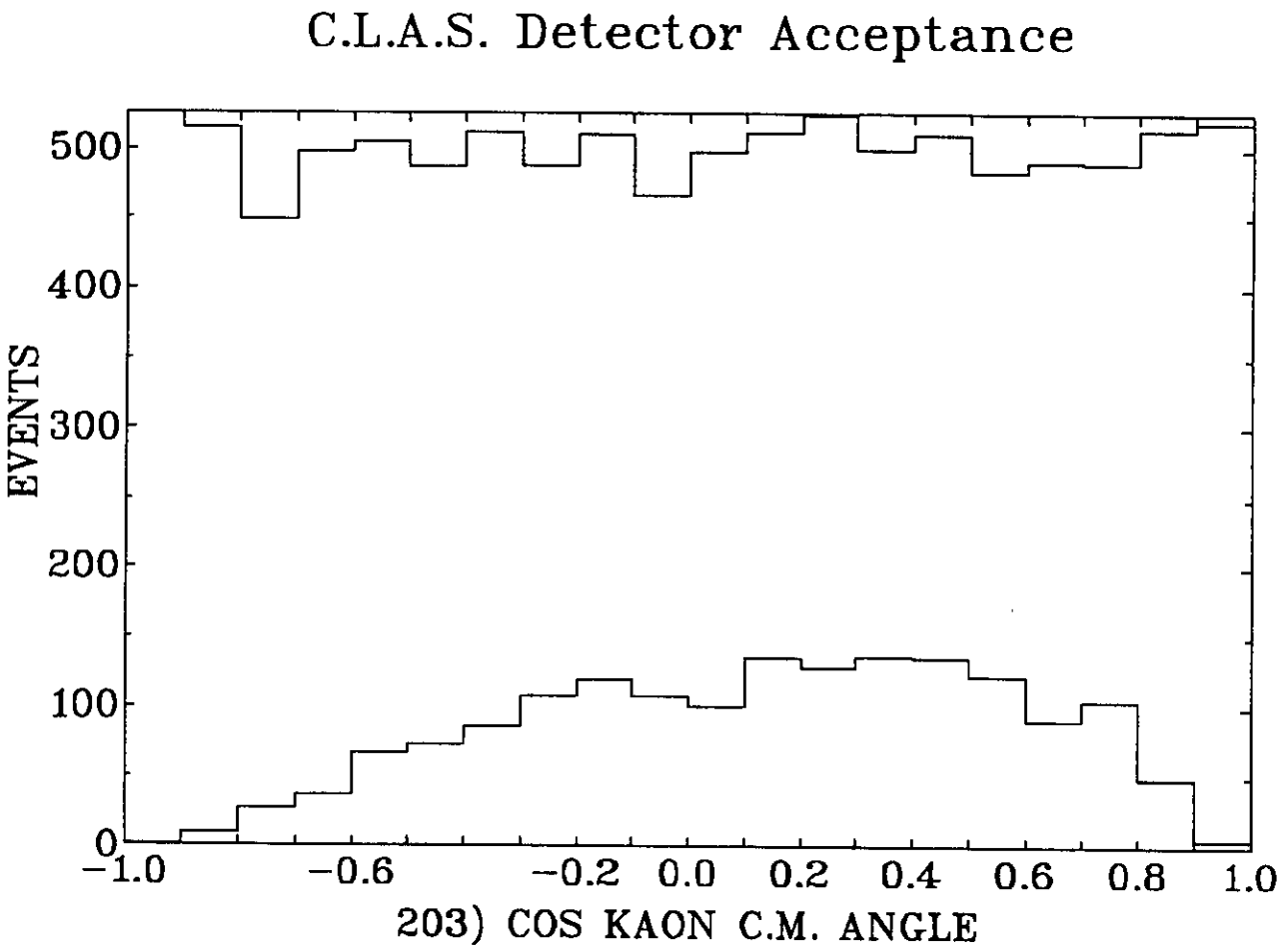
C.L.A.S. Detector Acceptance
EVENTS
500
400
300
200
100
0
−1.0
−0.6
−0.2
0.0
0.2
0.4
0.6
0.8
1.0
203) COS KAON C.M. ANGLE
Time: 18−OCT−89 09:07:05; File: FASTGK.HBK

Figure 15

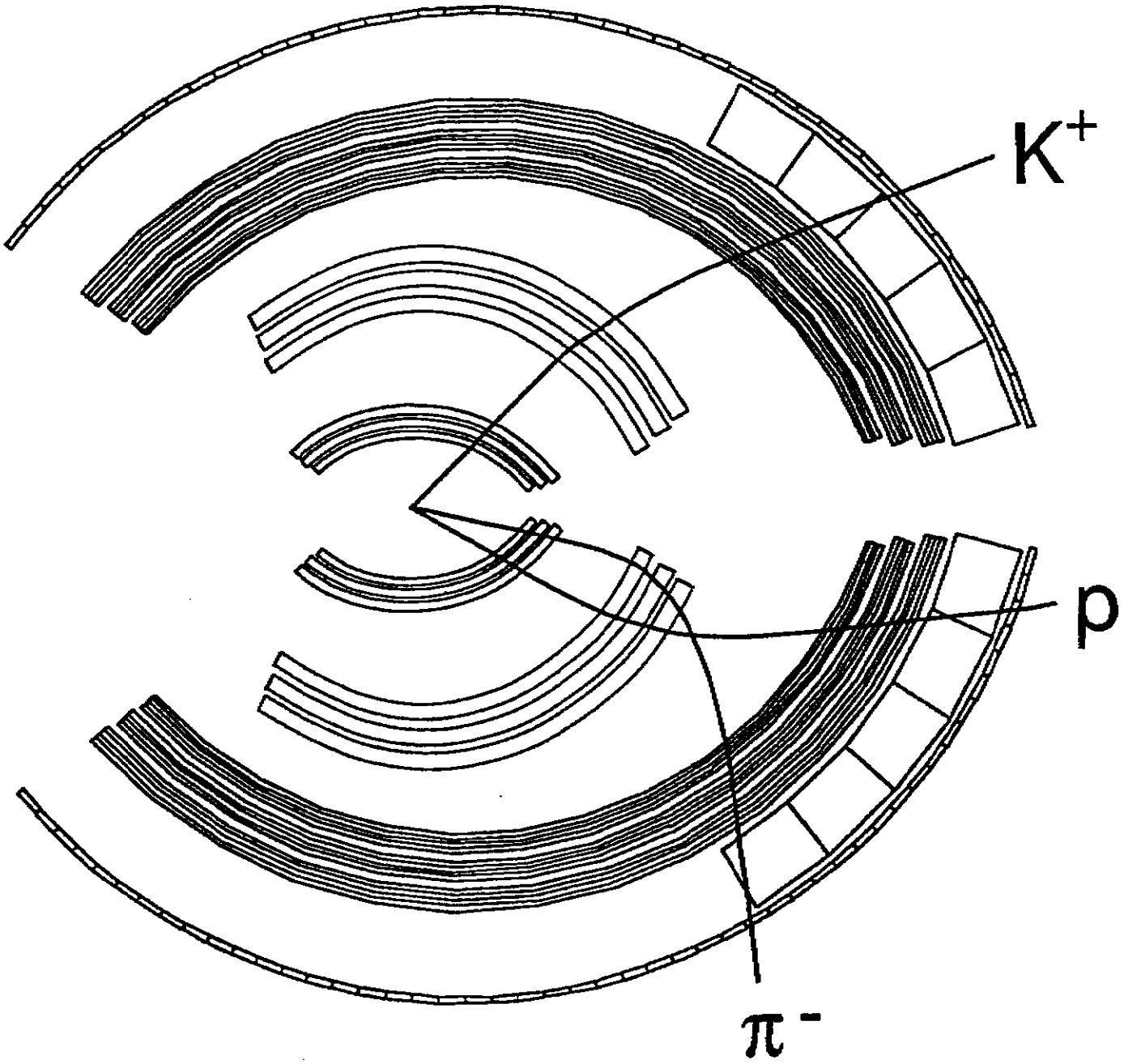

DENNIS 01 27KF

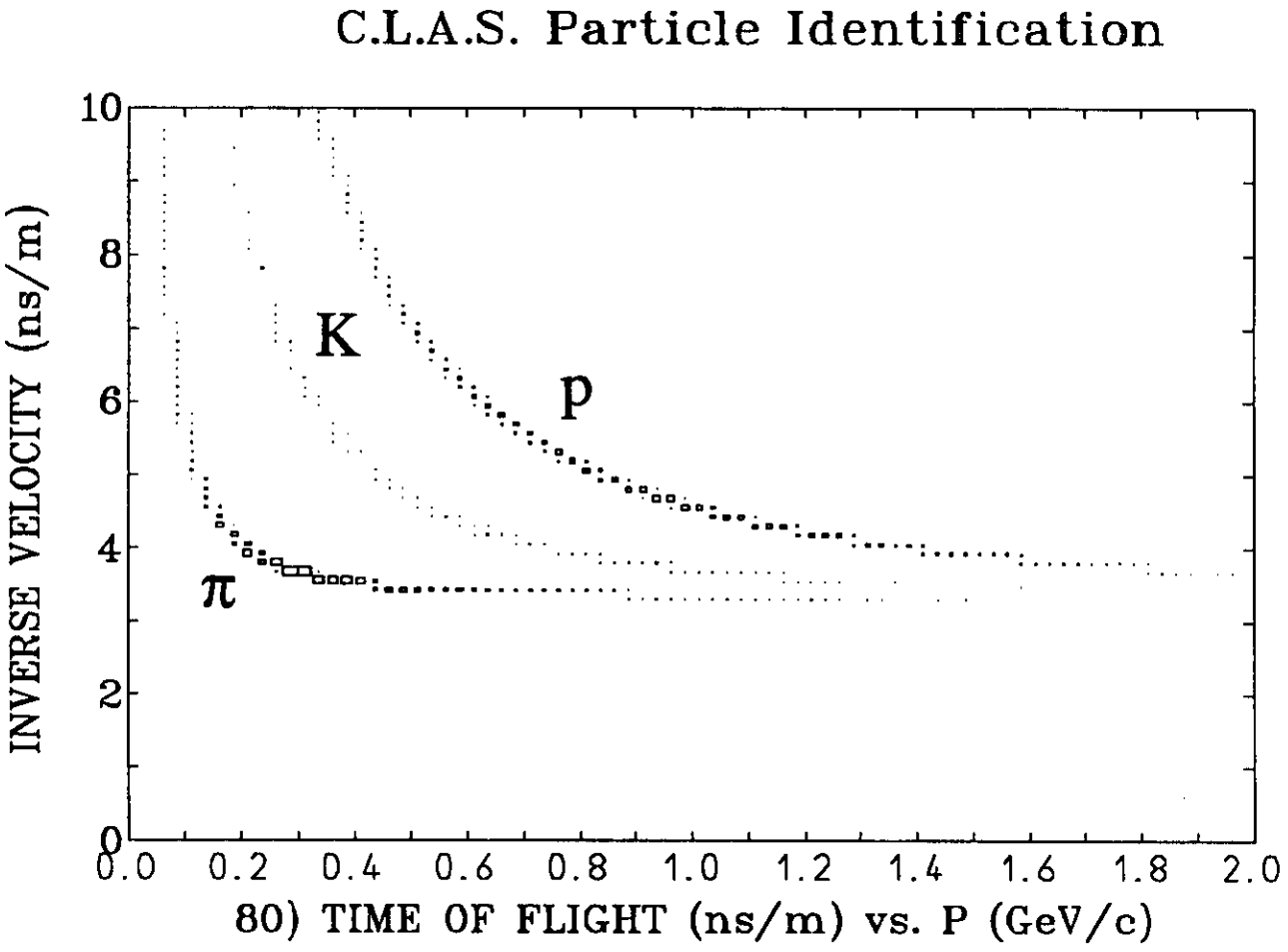
C.L.A.S. Particle Identification
INVERSE VELOCITY (ns/m)
10
8
6
4
2
0
K
p
π
0.0
0.2
0.4
0.6
0.8
1.0
1.2
1.4
1.6
1.8
2.0
80) TIME OF FLIGHT (ns/m) vs. P (GeV/c)
Time: 20-OCT-89 17:58:40; File: FASTGK.HBK

Figure 17

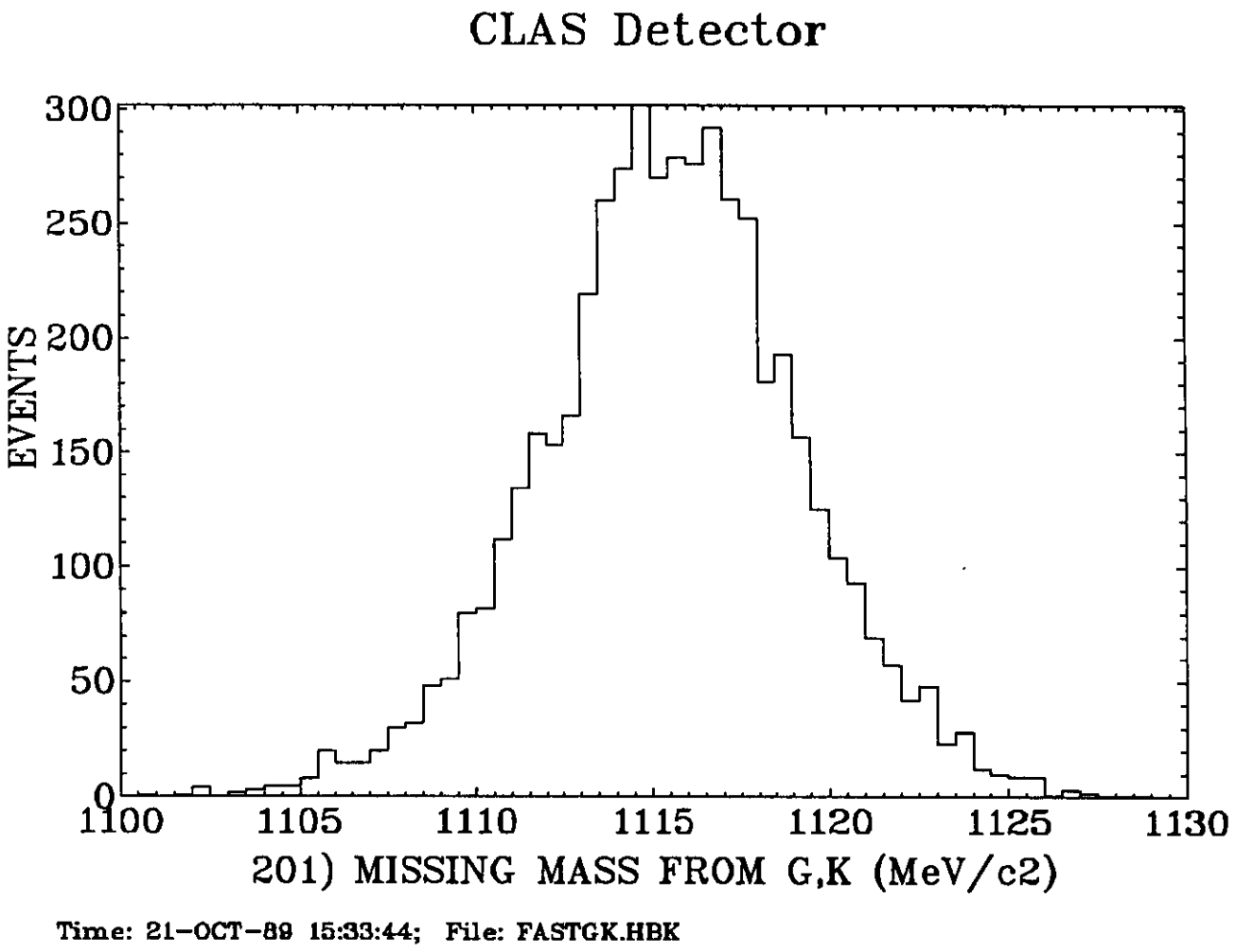
CLAS Detector
EVENTS
300
250
200
150
100
50
0
1100
1105
1110
1115
1120
1125
1130
201) MISSING MASS FROM G,K (MeV/c2)
Time: 21-OCT-89 15:33:44; File: FASTGK.HBK

Figure 18

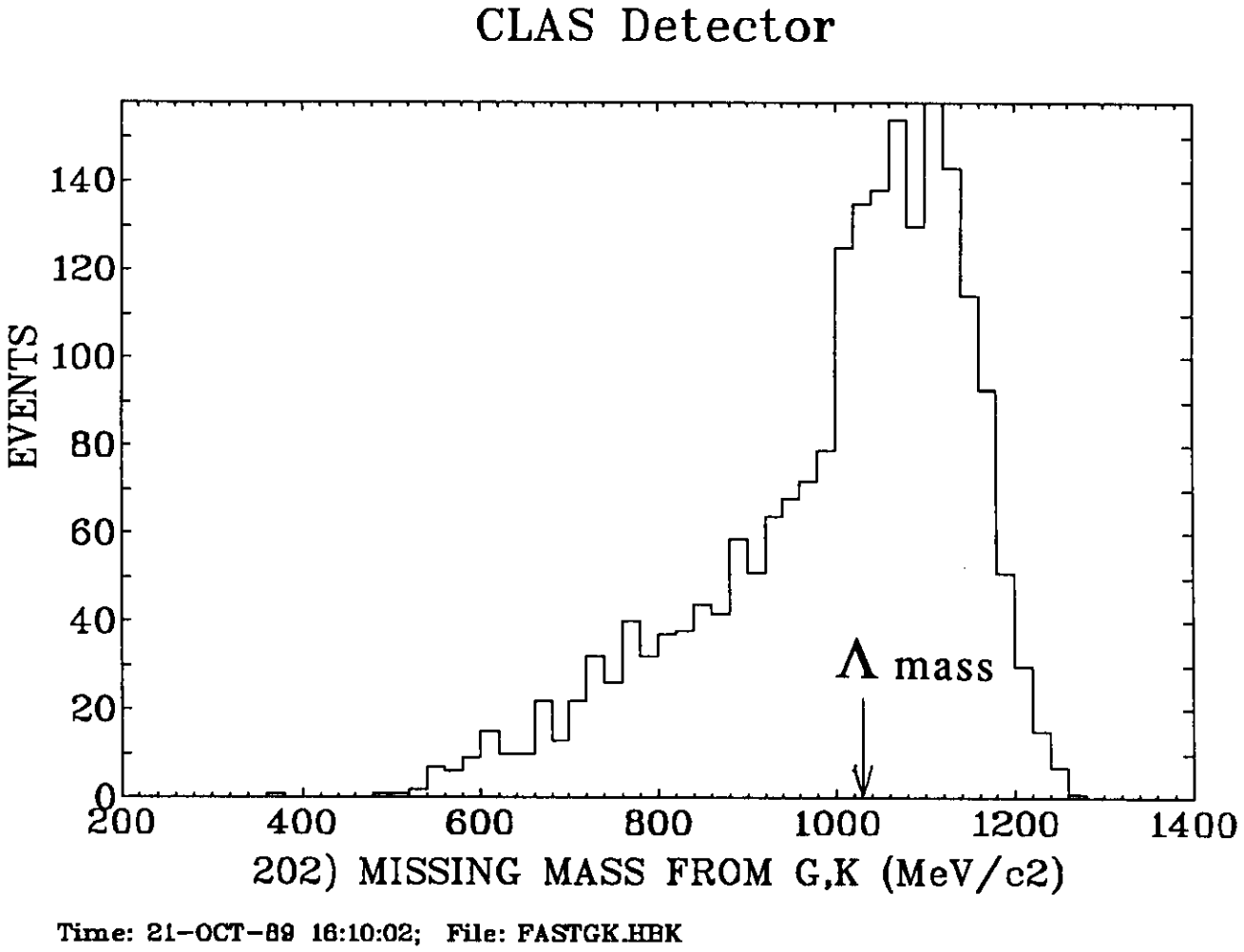
CLAS Detector
EVENTS
140
120
100
80
60
40
20
0
200
400
600
800
1000
1200
1400
Λ mass
202) MISSING MASS FROM G,K (MeV/c2)
Time: 21-OCT-89 16:10:02; File: FASTGK.HBK

Figure 19

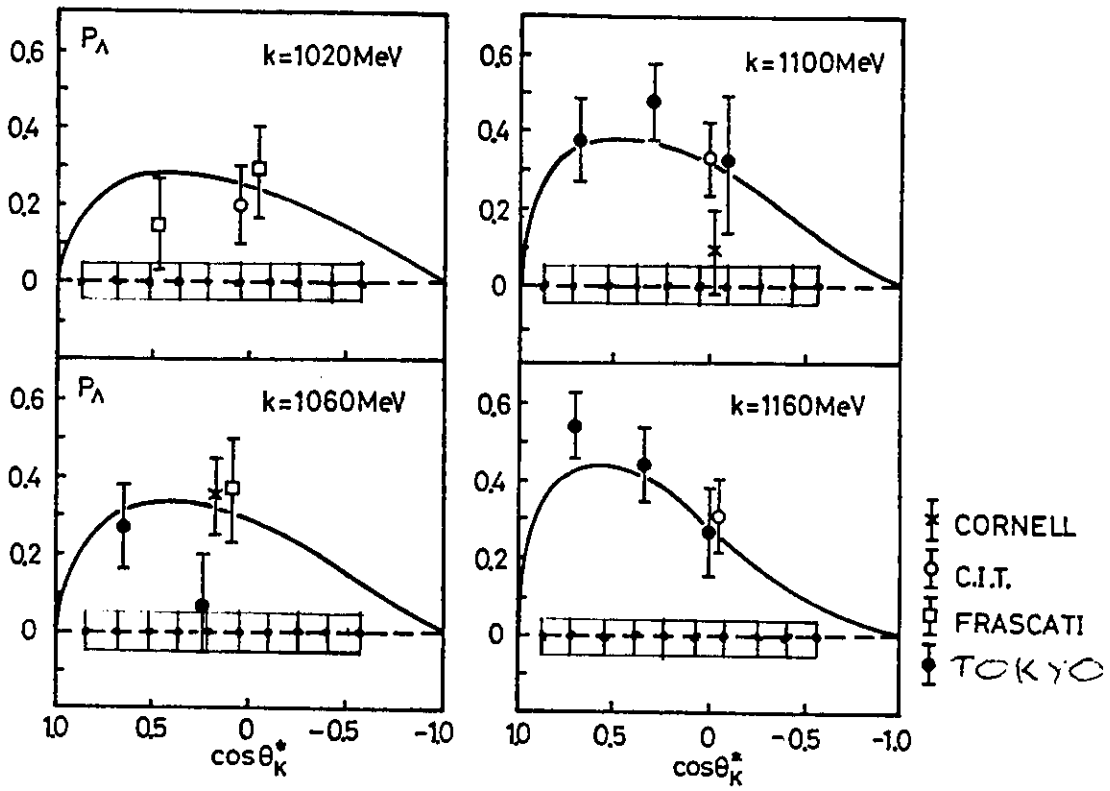
P_Λ
k=1020MeV
k=1100MeV
k=1060MeV
k=1160MeV
0.6
0.4
0.2
0
1.0
0.5
0
-0.5
-1.0
cosθ*K
CORNELL
C.I.T.
FRASCATI
TOKYO

Figure 20

Continuous Electron Beam Accelerator Facility

12000 Jefferson Avenue
Newport News, Virginia 23606
(804) 249-7100

Proposal Number: PR-89-004

Proposal Title: Electromagnetic Production of Hyperons

Spokespersons/Contact Persons: R. Schumacher

Proposal Status at CEBAF:

Approval for 30 days of running, with the understanding that the proponents of experiment PR-89-024 be participants and have access to the data relevant to their proposed measurements. Modifications to accommodate PR-89-024 are encouraged as long as they do not compromise this measurement. The PAC will review progress at a future meeting.

Dirk Walecka

John Dirk Walecka
Scientific Director